TEOS-10 and the Climatic Relevance of Ocean-Atmosphere Interaction

Rainer Feistel

Leibniz Institute for Baltic Sea Research (IOW), 18119 Warnemünde, Germany

Correspondence: Rainer Feistel (rainer.feistel@io-warnemuende.de)

Abstract: Unpredicted observations in the climate system, such as recently an excessive ocean warming, are often lacking immediate causal explanations and are challenging the numerical models. As a highly advanced mathematical tool, the Thermodynamic Equation of Seawater – 2010 (TEOS-10) had been established by international bodies as an interdisciplinary standard and is recommended for use in geophysics, such as especially in climate research. From its very beginning, the development of TEOS-10 was supported by *Ocean Science* through publishing successive stages and results. Here, history and properties of TEOS-10 are briefly reviewed. With focus on the air-sea interface, selected current problems of climate research are discussed and tutorial examples for the possible use of TEOS-10 in the associated context are presented, such as related to ocean heat content, latent heat and rate of marine evaporation, properties of sea spray aerosol, or climatic effects of low-level clouds. Appended to this article, a list of publications and their metrics is provided for illustrating the uptake of TEOS-10 by the scientific community, along with some continued activities, addressing still pending, connected issues such as uniform standard definitions of uncertainties, of relative humidity, seawater salinity or pH.

This article is dedicated to the Jubilee celebrating 20 years of Ocean Science.

All the rivers run into the sea; yet the sea is not full;
unto the place from whence the rivers come, thither they return again.
The King James Bible: Ecclesiastes, 450 - 150 BCE

He wraps up the waters in his clouds,
yet the clouds do not burst under their weight.
Holy Bible: New International Version, Job 26:8

Of the air, the part receiving heat is rising higher.
So, evaporated water is lifted above the lower air.
Leonardo da Vinci: Primo libro delle acque, Arundel Codex, ca. 1508

Two-thirds of the Sun's energy falling on the Earth's surface is needed
to vaporize ... water ... as a heat source for a gigantic steam engine.
Heinrich Hertz: Energiehaushalt der Erde, 1885

The sea surface interaction is obviously
a highly significant quantity in simulating climate.
Andrew Gilchrist, Klaus Hasselmann: Climate Modelling, 1986

The climate of the Earth is ultimately determined
by the temperatures of the oceans.
Donald Rapp: Assessing Climate Change, 2014

1 Introduction

42 Quite recently in 2024, climate research has published alarming news: "The world's oceans absorbed
43 more heat in 2023 than in any other year since records began in the 1950s. … Data show that the
44 heat stored in the upper 2,000 metres of oceans increased by 15 zettajoules (1 zettajoule is 10^{21}
45 joules) in 2023 compared with that stored in 2022. This is an enormous amount of energy — for
46 comparison, the world's total energy consumption in 2022 was roughly 0.6 zettajoules" (You 2024: p.
47 434). Dividing this value by the global ocean surface area and by the duration of a year, the reported
48 ocean's average warming rate amounts to 1.3 W m^{-2}, and is apparently even counting. "The drivers
49 of a larger Earth energy imbalance in the 2000s than [before] are still unclear. … Future studies are
50 needed to further explain the drivers of this change" (von Schuckmann et al. 2023). Laterally, the
51 observed heat excess is unevenly distributed over the world ocean (Fig. 1), in contrast to what
52 naively may be expected from rising atmospheric CO_2 concentrations. Rather, warming seems to be
53 most pronounced in the austral and boreal west-wind belts.
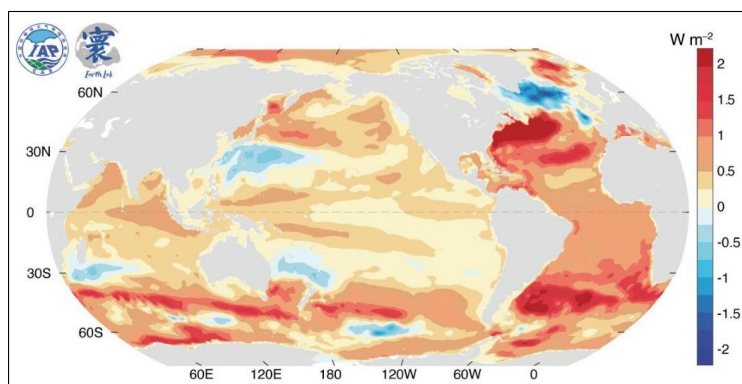
54

55 Fig. 1: Observed trend 1958 through 2022 of the upper 2000 m ocean heat content (WMO 2024).
56 Image reproduction permitted by WMO Copyright.

57

58 Sunlight is the only available heat source of sufficient power to cause the observed warming, while
59 the globally averaged geothermal heat flux is estimated to be just 0.087 W m^{-2} (Pollack et al. 1993),
60 and is not expected to suddenly rise recently due to human impact. Irradiation is hampered by
61 clouds, dust and absorbing gases, and water surface reflection such as by whitecaps, waves or
62 plankton layers. Heat absorbed in the water column may effectively exit the ocean again only across
63 the air-sea interface via sensible, radiative and latent heat flux. All these effects may vary in the
64 climate system in a complicated, mutually interacting manner. Typically, present numerical climate
65 models suffer from an "ocean heat budget closure problem" (Josey et al. 1999) and describe the
66 ocean-atmosphere heat flux only to within uncertainties between 10 W m^{-2} and 30 W m^{-2} (Josey et
67 al. 2013). According to recent model comparison studies, many of those "models fail to provide as
68 much heat into the ocean as observed" (Weller et al. 2022: p. E1968). Dynamical models, rather than
69 observed correlations, are the most reliable tools for the detection and verification of causal
70 relations (Feistel 2023), however, such as in this case of air-sea interaction, large uncertainties may
71 prevent any significant conclusions to be drawn regarding the causes of the observed ocean warming
72 rate of 1.3 W m^{-2}.

73 Of the increasing amount of water vapour contained in the global troposphere, 85 % result from
74 ocean evaporation (Gimeno et al. 2013). Corresponding to 1200 mm annual evaporation

75 (Baumgartner and Reichel 1975, Peters-Lidard et al. 2019), the associated latent heat flux of about 95
76 W m^{-2} per ocean surface area represents the strongest energy supply for the atmospheric dynamics
77 (Albrecht 1940) and at the same time the strongest cooling process of the sea. This flux depends
78 sensitively on the relative humidity (RH) at the water surface; an RH increase by 1 %rh can be
79 estimated to reduce evaporation by 5 W m^{-2} (Feistel 2015, Feistel and Hellmuth 2021, 2023), so that
80 minor additional 0.2 %rh may already suffice to warm up the ocean by the observed 1.3 W m^{-2}.
81 Unfortunately, marine RH is observed only with uncertainties between 1 and 5 %rh (Lovell-Smith et
82 al. 2016), or, accordingly, between 5 and 25 W m^{-2} of latent heat flux. It remains unclear to what
83 extent minor, yet unnoticed changes in marine RH may be responsible for the recent ocean warming.
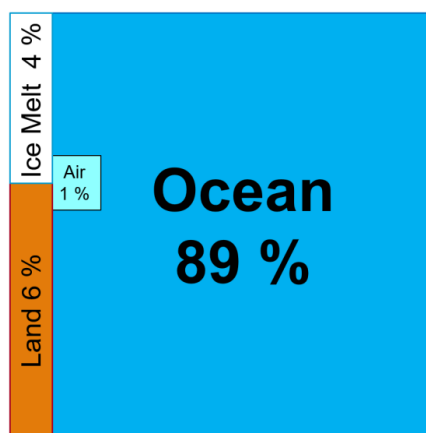
84

85 Fig. 2: Heat fractions stored additionally in the different parts of the Earth system 1960–2020 (values
86 from von Schuckmann et al. 2023), represented graphically by partial areas. Obviously, the oceans
87 dominate global warming.

88

89 According to Fig. 2, a paramount share of 94 % of global warming occurs in different phases and
90 geophysical mixtures of water, in particular in seawater. Considering this situation, the *Scientific*
91 *Committee on Oceanic Research* (SCOR) in cooperation with the *International Association for the*
92 *Physical Sciences of the Oceans* (IAPSO) decided at its 2005 Cairns meeting the establishment of the
93 *SCOR/IAPSO Working Group 127 on Thermodynamics of Seawater* (Millero 2010, Pawlowicz et al.
94 2012), which held its inaugural meeting in 2006 at Warnemünde (Fig. 3). It had been recognised that
95 "modeling of the global heat engine needs accurate expressions for the entropy, enthalpy, and
96 internal energy of seawater so that heat fluxes can be more accurately determined in the ocean"
97 (Millero 2010: p. 28) while such properties were not available from the thermodynamic seawater
98 standard at that time, the 1980 Equation of State of Seawater (EOS-80) (Fofonoff and Millard Jr.
99 1983).

100 The foundation of WG127 happened almost coincidently with the establishment of the *Ocean*
101 *Science* journal of the *European Geosciences Union* (EGU) in 2004/05. The development of the new
102 standard by WG127, the Thermodynamic Equation of Seawater – 2010 (TEOS-10) was very
103 successfully supported by Ocean Science, publishing the Special Issue #14 on "Thermophysical
104 Properties of Seawater" with 16 articles between 2008 and 2012 (Feistel et al. 2008a). **Appendix A**
105 reports the current metrics of this Special Issue. Also in 2008, at its conference in Berlin, Germany,
106 the *International Association for the Properties of Water and Steam* (IAPWS) established a new
107 *Subcommittee on Seawater* (SCSW) that cooperated closely with WG127. In the form of carefully

108 verified mathematical formulations for properties of water, ice, seawater and humid air, IAPWS
109 adopted 9 fundamental documents related to TEOS-10 (IAPWS AN6-16 2016), see **Appendix A**.

110

111 Fig. 3: Participants of the 2006 kick-off meeting of SCOR/IAPSO WG127 at the Leibniz Institute for
112 Baltic Sea Research (IOW) in Warnemünde, Germany. From left to right: Chen-Tung Arthur Chen
113 (Taiwan), Frank Millero (USA), Brian King (UK), Rainer Feistel (WG vice chair, Germany), Daniel Wright
114 (Canada, deceased 2010), Trevor McDougall (WG chair, Australia) and Giles Marion (USA).

115

116 Fig. 4: Participants of the BIPM-IAPWS meeting in February 2012 at the Pavillon de Breteuil, Sèvres.
117 From left to right: Dan Friend (IAPWS), Karol Daučik (IAPWS president), Jeff Cooper (IAPWS), Alain
118 Picard (BIPM, deceased 2015), Petra Spitzer (WG127), Rainer Feistel (WG127), Michael Kühne
119 (director BIPM), Andy Henson (BIPM), Robert Wielgosz (BIPM).

120

121 With respect to problems yet pending after the official adoption of TEOS-10, especially for the
122 preparation of future novel international definitions of seawater salinity, seawater pH and
123 atmospheric relative humidity (Feistel et al. 2016, Pawlowicz et al. 2016, Dickson et al. 2016, Lovell-
124 Smith et al. 2016), the standing *IAPSO/SCOR/IAPWS Joint Committee on the Properties of Seawater*
125 (JCS) was established in 2012. In 2011, IAPWS also extended its cooperation with the *International*
126 *Bureau for Weights and Measures* (BIPM), see Fig. 4. Further details on TEOS-10 (IOC et al. 2010,
127 McDougall et al. 2013, Feistel 2018, Wikipedia 2024) are available from the TEOS-10 homepage,
128 www.teos-10.org, and are briefly reviewed in **Section 2** and **Appendix B**.

129 In the context of the predecessor EOS-80, the *ocean heat content* (OHC) was defined in terms of
130 *potential temperature* (Abraham et al. 2013). Improving this method, TEOS-10 entropy and enthalpy
131 of seawater provided a proper quantitative basis for a novel, thermodynamically rigorous definition

132 of the OHC in the form of seawater *potential enthalpy* (McDougall 2003, McDougall et al. 2013,
133 Graham and McDougall 2013, McDougall et al. 2021), equivalently defined as *conservative*
134 *temperature* and briefly discussed in **Section 3**.

135 Currently implemented parameterisations of marine evaporation rates in the form of historical
136 *Dalton equations* (Stewart 2008, Josey et al. 2013) may be replaced by TEOS-10 chemical potentials
137 which provide the proper quantitative basis for a thermodynamically rigorous formulation of non-
138 equilibrium Onsager forces and fluxes in terms of *relative fugacity* (RF) of humid air (Kraus and
139 Businger 1994, Feistel and Lovell-Smith 2017, Feistel and Hellmuth 2023, 2024a), as described in
140 **Section 4.** *Relative humidity* (RH) is defined relative to the saturation state of moist air, which in turn
141 is controlled by the chemical potentials of water in the gas and liquid phase. It is only natural,
142 therefore, to define RH in terms of chemical potentials, which in fact is performed by RF. The
143 uncertainty of latent heat flux with respect to the uncertainty of surface RH observation is shown to
144 be significantly larger than the observed warming of 1.3 W m^{-2}, so that this warming may or may
145 not be caused by so-far ignored minor RH increase.

146 The conceptual model of sea air as a two-phase composite thermodynamic system is outlined in
147 **Section 5**. The roles of enthalpy, chemical potential and entropy are explained by means of explicit
148 theoretical descriptions of three simplified tutorial examples, (i) for the latent heat of evaporation,
149 (ii) for the heat capacity of humid air containing sea spray, and (iii) for the entropy production of
150 irreversible evaporation.
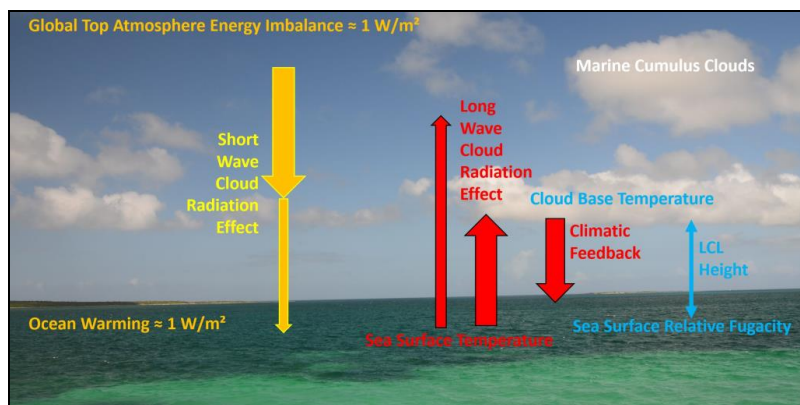
151

152 Fig. 5: Schematic of *cloud radiation effects* (CRE). The *short-wave effect* (SW CRE) controls the
153 downward flux of solar irradiation while the *long-wave effect* governs the infrared radiation balance
154 between water surface and cloud base. By thermal convection, cumulus clouds emerge at the
155 isentropic *lifted condensation level* (LCL). Figure from Feistel and Hellmuth (2024b)

156

157 Clouds do not only release the latent heat which water vapour has carried away from the ocean, they
158 also interfere substantially in the global radiation balance, cooling the surface by reflecting short-
159 wave solar irradiation, and warming the surface by sending back down long-wave thermal radiation,
160 see Fig. 5. In the course of global warming, cloudiness has been found to exhibit a systematic trend of
161 reduction, see **Section 6**, which affects the ocean heat content in a non-trivial, non-uniform manner.
162 Marine cumulus clouds form by isentropic uplift of thermal convection. Their height controls their
163 temperature and thermal downward radiation, affecting the ocean's energy balance. Updating
164 previous results (Romps 2017) for the *lifted condensation level* (LCL) of marine cumulus clouds to
165 thermodynamically rigorous TEOS-10 standard equations (Feistel and Hellmuth 2024b), the radiative

166 effect of those clouds can be estimated from *sea-surface temperature* (SST) and surface relative
167 humidity. This effect turns out to be weakly cooling and cannot provide a reasonable explanation for
168 the so-far unclear strong ocean warming.

169 **Section 7** provides a summery of this paper, **Appendix A** reports collections of publications with
170 respect to TEOS-10 as well as their metrics, and **Appendix B** offers a short introduction into the
171 concept of thermodynamic potentials.

172

173 ## 2 Thermodynamic Equation of Seawater – 2010 (TEOS-10)

174 In the climate system, the omnipresent and dominant substance is water in various phases and
175 mixtures. For example, "water vapor is by far the most important greenhouse gas, in the sense that it
176 absorbs more irradiance from the Earth than all other greenhouse gases combined" (Rapp 2014: p.
177 381). Textbooks and other publications offer numerous collections of various different property
178 equations for water, ice, seawater or moist air, but uncertainties and mutual consistencies of those
179 equations are often unclear. To improve this situation, a novel *Thermodynamic Equation of Seawater
180 – 2010* (TEOS-10) was developed by the members of the SCOR/IAPSO Working Group 127 (WG 127)
181 in close cooperation with the International Association for the Properties of Water and Steam
182 (IAPWS). TEOS-10 is described in a detailed Manual (IOC et al. 2010) and has been adopted and
183 recommended by IOC-UNESCO (2009) in Paris and by the IUGG (2011) in Melbourne, see also Feistel
184 (2008b, 2012, 2018), Valladares et al. (2011) and Pawlowicz et al. (2012). Starting in 2008 with a
185 Special Issue of *Ocean Science* (Feistel et al. 2008a), a large number of scientific publications has
186 appeared in the meantime, supporting, extending or exploiting TEOS-10. A collection of selected
187 papers related to TEOS-10 is summarised in Appendix A together with metrics that illustrate the
188 growing uptake of TEOS-10 by the scientific community.

189 The development of the first numerical thermodynamic Gibbs potentials (see Appendix B) for
190 seawater (Feistel 1991, 1993, Feistel and Hagen 1995) was based on the works of Millero and Leung
191 (1976) and Millero (1982, 1983), together with high-pressure background data of the previous EOS-
192 80 standard (Unesco 1981). Independently of that, a Helmholtz potential for pure fluid water had
193 been adopted by IAPWS in 1996 at Fredericia (Harvey 1998, Wagner and Pruß 2002). These were the
194 key activities which eventually culminated in the formulation of TEOS-10 about two decades later. By
195 combining those equations for pure and seawater, some known pending problems of EOS-80
196 (Fofonoff and Millard Jr. 1983) could incidentally be resolved (Feistel 2003). In the end, TEOS-10 has
197 been assembled from four basic thermodynamic potentials derived from mutually consistent, most
198 comprehensive and accurate datasets of measured properties available at that time. Those
199 potentials are:

200 (i)   A Helmholtz function of fluid water, $f^{\mathrm{F}}(T,\rho) \equiv f^{\mathrm{W}}(T,\rho) \equiv f^{\mathrm{V}}(T,\rho)$, known as the
201   IAPWS-95 formulation (Wagner and Pruß 2002), which is identical for liquid water,
202          $f^{\mathrm{W}}(T,\rho)$ and for water vapour, $f^{\mathrm{V}}(T,\rho)$. It describes de-aerated water of a fixed
203   isotopic composition, termed *Standard Mean Ocean Water* (SMOW).
204

205 (ii)   A Gibbs function of ambient hexagonal ice I, $g^{\mathrm{Ih}}(T,p)$, or IAPWS-06 formulation (Feistel
206   and Wagner 2006), see Tables A2 and A3 of Appendix A.
207

208 (iii)   A Gibbs function of *IAPSO Standard Seawater*, $g^{\mathrm{SW}}(S,T,p)$, or IAPWS-08 formulation
209   (Feistel 2008a), see Tables A2 and A3 of Appendix A. The variable S, at which a subscript
210   A is omitted here for simplicity, is the specific or *absolute salinity*, the mass fraction of

211   dissolved salt in seawater, which differs from practical salinity, S_P, measured by
212   oceanographic instruments (Millero et al. 2008). Sea salt is assumed to have
213   stoichiometric *Reference Composition*. The pure-water limit, $g^{SW}(0,T,p) = g^W(T,p)$, is
214   the Gibbs function of liquid water computed from the IAPWS-95 Helmholtz function
215    $f^W(T,\rho)$. For brackish seawater, g^{SW} has implemented Debye's root law of dilute
216   electrolyte solutions (Landau and Lifschitz 1966, Falkenhagen et al. 1971).

218   (iv)   A Helmholtz function of humid air, $f^{AV}(A,T,\rho)$, or IAPWS-10 formulation (Feistel et al.
219   2010a), see Tables A1 and A2 of Appendix A. The variable A is the mass fraction of dry air
220   admixed with water vapour, so that $q = 1 - A$ is the *specific humidity*. The dry-air limit
221            $f^{AV}(1,T,\rho) = f^A(T,\rho)$ equals, up to modified reference-state conditions, the equation
222   of state of Lemmon et al. (2000). The air-free limit $f^{AV}(0,T,\rho) = f^V(T,\rho)$ equals the
223   IAPWS-95 Helmholtz function. In f^{AV}, the interaction of water vapour with dry air is
224   described by 2nd and 3rd virial coefficients.

226   Thermodynamic potentials include certain adjustable constants expressing the absolute energies and
227   entropies of the particular substances, which are not available from measurement (Planck 1906,
228   Feistel 2019) and have, in turn, no effect on measurable properties derived from those potentials.
229   The TEOS-10 reference states (Feistel et al. 2008b, 2010a) are the triple point of water, $T_{TP} =$
230   273.16 K, $p_{TP} = 611.654\ 771$ Pa, where the conditions

232    $$\eta^W_{TP} = 0, \qquad e^W_{TP} = 0, \tag{1}$$

234   are imposed, and the standard ocean state, $S_{SO} = 35.165\ 04$ g kg^{-1}, $T_{SO} = 273.15$ K, $p_{SO} =$
235   101 325 Pa, with the conditions for sea salt,

237    $$\eta^{SW}_{SO} = 0, \qquad h^{SW}_{SO} = 0, \tag{2}$$

239   and for dry air,

241    $$\eta^A_{SO} = 0, \qquad h^A_{SO} = 0. \tag{3}$$

243   Here, η, e and h, respectively, are specific entropy, internal energy and enthalpy of those substances.
244   The TEOS-10 potential functions and properties derived thereof are numerically implemented in two
245   different libraries, the Sea-Ice-Air (SIA) and the Gibbs-Seawater (GSW) libraries, see Table A4 in
246   Appendix A.

248   The SIA library includes empirical coefficients only in the four fundamental potentials (Feistel 2010d,
249   Wright et al. 2010). All other potential functions and properties are derived strictly by mathematical
250   operations to ensure consistent results, even at the cost of low computation speeds as a result of
251   stacked iteration procedures. All quantities are exclusively expressed in basic SI units such as kg, m, J
252   or Pa. A more recent extension of SIA code is reported in Feistel et al. (2022) for the computation of
253   relative fugacity.

255   The GSW library is tailored for oceanographic models, optimised in computation speed (Roquet et al
256   2015). For fast numerical evaluation, GSW procedures contain new empirical coefficients determined
257   from the SIA library functions by regression. Units and variables are adjusted to common
258   oceanographic practice such as pressure in decibars relative to surface pressure, or temperatures in

259 °C. *Conservative Temperature* (CT) is used as a new preferred thermal variable. An additional
260 thermodynamic potential has been constructed (McDougall et al. 2023) that supports the use of CT
261 universally as an independent variable.

262

263   3   Potential Enthalpy and Ocean Heat Content (OHC)

264 Thermodynamically, the term "Ocean Heat Content" (OHC) is a sloppy wording. "Content" means a
265 state quantity of a body or volume while, however, "heat" is an exchange quantity rather than a
266 state quantity. "The obsolete hypothesis of heat being a substance is excluded" (Sommerfeld 1988:
267 p. 6). This distinction is qualitatively fundamental (Feistel 2023). Physical conservation quantities
268 such as energy or mass have the key property that the change of that quantity in a volume equals the
269 flux of that quantity across the boundary (Landau and Lifschitz 1966, Glansdorff and Prigogine 1971),
270 but this does not apply to "heat". For example, a heat engine receives a permanent net heat flux
271 without getting permanently hotter. While asking how much "heat" is contained in the ocean may
272 find ambiguous answers, it is well defined to say how much heat has entered of left the ocean across
273 its boundary by a specified process that transfers the ocean from a certain state of reference to the
274 current state of interest. In this section, based upon TEOS-10, related states and processes are
275 described which may properly specify what is commonly termed OHC. This consideration intrinsically
276 connects OHC with ocean-atmosphere exchange processes relevant for climate change.

277 Since a long time, measuring and calculating the ocean's "heat" has been a question of central
278 interest to oceanography. Recently, this issue has become even more important and urgent in the
279 context of climate change. "The total energy imbalance at the top of atmosphere is best assessed by
280 taking an inventory of changes in energy storage. The main storage is in the ocean" (Abraham et al.
281 2013: p. 450). The conventional approach is a formally defined mathematical procedure based on
282 potential temperatures. "Changes to ocean heat content (OHC) can be calculated from
283 measurements of the temperature evolution of the ocean. The OHC is attained from the difference
284 of the measured potential temperature profile and the potential temperature climatology. This
285 difference is integrated over a particular reference depth (for instance, 700 m) and is multiplied by a
286 constant ocean density reference and heat capacity" (Abraham et al. 2013: p. 468). However, this
287 OHC definition has no rigorous thermodynamic justification, and the relation to processes of ocean-
288 atmosphere heat fluxes is not entirely clear. If a sea-air heat flux of 1 W m^{-2} warms up the
289 atmosphere, by what rate exactly will that OHC decrease?

290 Making the seawater properties entropy and enthalpy quantitatively available, TEOS-10 has offered a
291 thermodynamically improved option for defining OHC (McDougall et al. 2021), in the form of the
292 integral over the ocean volume,

293 $$OHC = \int h^{SW}(S, \eta, p_0)\, \rho^{SW}(S, \eta, p)\mathrm{d}V\,. \tag{4}$$

294 Here, $h^{SW}(S, \eta, p_0)$ is the *potential enthalpy* (McDougall 2003) relative to the surface pressure, p_0,
295 and $\rho^{SW}(S, \eta, p)$ is the in-situ mass density at the pressure p of a parcel with salinity and entropy
296 equal to those before. This definition can be understood in terms of both, a specified process of heat
297 exchange, and a reference state relative to which OHC is counted, as follows:

298   (i)   A virtual **heat exchange process** supporting the definition (4) is sketched in Fig. 6. In turn,
299   each ocean parcel with in-situ properties (S, η, p) is lifted to the surface pressure p_0,
300   keeping its salinity and entropy constant. There, it reversibly exchanges heat, $\mathrm{d}h = T\mathrm{d}\eta$,
301   with a measuring device until the parcel's entropy has reached a certain reference value,
302   η_{ref}, while the parcel's salinity remains unchanged. Subsequently, the heat is reversibly

303 put back to the parcel which is then returned to its original location. The work required
304 to lift and lower the parcel is balanced.

305 (ii) The **reference state** relative to which OHC is measured is arbitrary and may be chosen by
306 convenience or usefulness. In eq. (4), this state is defined by η_{ref} which satisfies
307 $h^{\mathrm{SW}}(S, \eta_{\mathrm{ref}}, p_0) = 0$.

308 An alternative choice for the reference value of entropy, up to which the heat exchange with the
309 surface instrument is performed, could be $\eta_{\mathrm{ref}} = 0$, in which case the definition (4) became

310 $$OHC^* = \int \left[h^{\mathrm{SW}}(S, \eta, p_0) - h^{\mathrm{SW}}(S, 0, p_0) \right] \rho^{\mathrm{SW}}(S, \eta, p) \mathrm{d}V. \qquad (5)$$

311 Because entropy is conserved during the vertical excursion processes, the latter reference state of
312 the ocean is given be zero entropy all over the volume. In the case of (4), the alternative reference
313 state is zero potential enthalpy (or zero Conservative Temperature, McDougall 2003) of all ocean
314 parcels.
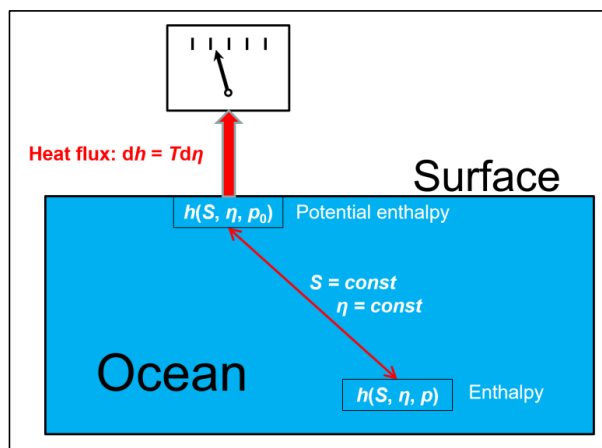
315

316 Fig. 6: Schematic of a conceptual process defining the ocean heat "content" (OHC) by measuring heat
317 flux across the ocean boundary according to eq. (4).

318

319 In a sense consistent with the previous OHC definition (Abraham et al. 2013), also a climatological
320 average state could in principle be chosen as the OHC reference. However, this option includes the
321 problem that the salinity distribution of the current ocean may differ from the reference ocean, and
322 that thermodynamically properly treating the required salt exchange processes at the surface may
323 turn the issue unnecessarily complicated.

324

325 **4 Relative Fugacity and Ocean Evaporation Rate**

326 In the past, several climate researchers have argued that along with global warming the marine
327 evaporation has or will be "amplified" or "intensified" (Feistel and Hellmuth 2021). However, it was
328 not always made clear whether this may mean that (a) in the course of a year, more water vapour is
329 transferred from the global ocean to the atmosphere, or (b) that the global mean evaporation rate
330 remains unchanged while locally or temporally, evaporation is more intense, or (c) any combination
331 of the two variants. Conclusions of kind (a) were drawn by renowned climatologists such as Budyko
332 (1984), Flohn et al. (1992), Yu (2007), Randall (2012) or Zhang et al. (2021).

333   By contrast, the currently observed ocean warming at a rate about 1 W m^{-2} does not support
334   assumptions of an enhanced hydrological cycle with related latent-heat cooling, rather, it more likely
335   suggests its slight reduction of evaporation. Two decades ago, Held and Soden (2006: p. 5687-89)
336   had already clearly stated that "it is important that the global-mean precipitation or evaporation,
337   commonly referred to as the strength of the hydrological cycle, does not scale with Clausius–
338   Clapeyron. … We can, alternatively, speak of the mean residence time of water vapor in the
339   troposphere as increasing with increasing temperature." Subsequent observations have underpinned
340   their statement.

341   Between 1979 and 2022, annual mean global precipitation values, see Figure 7, fluctuated by about
342   ± 10 mm yr^{-1}, in particular due to La Niña events, but do not exhibit a significant long-term trend
343   (Vose et al. 2023). Under the common assumption that global precipitation is balanced against
344   evaporation, no substantial strengthening of the hydrological cycle may be observed yet.
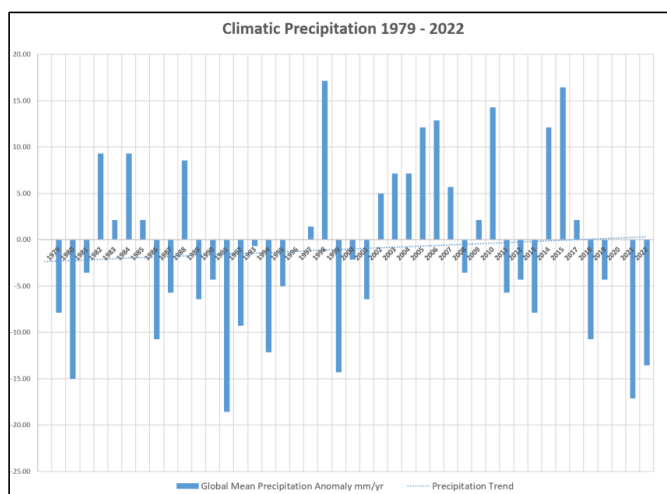
345

346   Fig. 7: Global mean precipitation anomaly 1979-2022 in mm yr^{-1}. The values displayed exhibit a minor
347   increasing trend (dotted line) of 0.06 mm yr^{-2}. Data from Vose et al. (2023)

348

349   Probably, the minor trend of 0.06 mm yr^{-2} of the data displayed in Fig. 7 is statistically insignificant.
350   Associated with this apparent trend, the latent heat transferred to the troposphere can be estimated
351   to a negligible putative warming rate of additional 0.5 mW m^{-2} per year, which could explain only 10
352   % of observed atmospheric warming by 1.7 °C per century (Morice et al. 2012, Feistel and Hellmuth
353   2021).

354   The thermodynamic driving force for evaporation is the difference between the chemical potentials
355   of water in humid air and in seawater at the two sides of the sea-air interface (Kraus and Businger
356   1994). TEOS-10 has made this difference numerically available in the form of the water mass
357   evaporation rate (Feistel and Hellmuth 2022, 2023)

358    $$J_{\mathrm{W}} = -D_f(u) \ln \frac{\psi_f}{x_{\mathrm{W}}}. \tag{6}$$

359   Here, $D_f(u)$, is an empirical transfer coefficient as a function of the wind speed, u, and x_{W} is the
360   mole fraction of water in seawater. Consistent with Wüst (1920), for the standard ocean with
361   Reference Composition, this fraction is (Millero et al. 2008: Table 4),

362 $\quad x_\mathrm{W} = \frac{53.556\ 514\ 4}{54.676\ 283\ 8} = 0.979\ 52.$ $\hspace{4cm}$ (7)

363 In eq. (6), the sea-surface humidity is expressed by the relative fugacity (RF), ψ_f, defined by the ratio
364 of the water-vapour fugacity in humid air, f_V, to that fugacity at saturation, $f_\mathrm{V}^\mathrm{sat}$ (Feistel and Lovell-
365 Smith 2017), see eq. (49). In ideal-gas approximation, RF equals conventional RH (Lovell-Smith et al.
366 2016)

367 $\quad \psi_f \equiv \frac{f_\mathrm{V}}{f_\mathrm{V}^\mathrm{sat}} \approx \psi_x \equiv \frac{x}{x^\mathrm{sat}}.$ $\hspace{4cm}$ (8)

368 Here, the mole fraction of water vapour in humid air is x, and its value at saturation is x^sat. Further,
369 ψ_x is the conventional definition of RF in metrology and meteorology (Lovell-Smith et al. 2016).
370 Independent of ideal-gas conditions, but sufficiently close to saturation, such as near the sea surface,
371 RF can be estimated in excellent approximation from the Clausius-Clapeyron formula (Feistel et al.
372 2022),

373 $\quad \psi_f \approx \exp\left\{\frac{L(T_\mathrm{dp}, p)}{R_\mathrm{W}}\left(\frac{1}{T} - \frac{1}{T_\mathrm{dp}}\right)\right\}.$ $\hspace{3cm}$ (9)

374 The evaporation enthalpy of pure water (IAPWS SR1-86 1992) at the dewpoint T_dp is L, and $R_\mathrm{W} =$
375 $461.523\ \mathrm{J\ kg^{-1}\ K^{-1}}$ is the specific gas constant of water. The typical marine RF is

376 $\quad \psi_f \approx 80\ \%\mathrm{rh},$ $\hspace{6cm}$ (10)

377 and is fairly independent of region, season or global warming (Dai 2006, Randall 2012, Rapp 2014,
378 MetOffice 2020). Indeed, observed ocean surface RH has no significant climatological trend (Willett
379 et al. 2023). Similarly, observed ocean wind speeds seem to be unaffected by global warming (Azorin-
380 Molina et al. 2023). Eq. (6) for the evaporation rate depends only on wind speed and RF, so that it
381 may be concluded that also the global mean evaporation rate has no significant climatic trend.
382 Hence, the TEOS-10 approach in the form of eq. (6) appears to be consistent with the prediction of
383 Held and Soden (2006).

384 Various empirical evaporation equations, commonly known as *Dalton equations*, are found in the
385 literature (Wüst 1920, Sverdrup 1936, 1937, Montgomery 1940, Debski 1966, Baumgartner and
386 Reichel 1975). Several numerical climate models estimate evaporation from the formula (Stewart
387 2008),

388 $\quad J_\mathrm{W} = D_q(u)(q_0 - q_{10}),$ $\hspace{5cm}$ (11)

389 where q_0 is the specific humidity at the sea surface and q_{10} is that at 10 m height, or from (Josey et
390 al. 1999, 2013)

391 $\quad J_\mathrm{W} = D_q(u)(0.98\ q^\mathrm{sat} - q).$ $\hspace{4cm}$ (12)

392 Here, q is the near-surface specific humidity, and q^sat is the saturation value at the same
393 temperature and pressure. The factor 0.98 accounts for the salinity, see eq. (7). After a few
394 approximation steps (Feistel and Hellmuth 2023), these Dalton equations can be derived from the
395 TEOS-version, eq. (6), however, there is an important qualitative difference. At constant RH, due to
396 global warming, specific humidities such as q and q^sat, as well as their difference, are increasing
397 following the Clausius-Clapeyron saturation formula. Accordingly, eq. (e4.6) implies that also the
398 evaporation rate J_W is growing this way, by contrast to eq. (6). This virtual acceleration of the
399 hydrological cycle is evidently inconsistent with the prediction of Held and Soden (2006). This
400 parameterisation-caused additional latent heat flux implies a spurious ocean cooling that may

401 contribute to the finding that many numerical climate models tend to underestimate the observed
402 ocean warming (Weller et al. 2022).

403 From eq. (6), the sensitivity of the latent heat flux, LJ_W, with respect to the RH variations is easily
404 estimated. For a mean evaporation rate of 1200 mm per year, the corresponding mass flux is about
405 $J_W \approx 3.8 \times 10^{-5}$ kg m^{-2}s^{-1} and the related heat flux is $LJ_W \approx 95$ W m^{-2} with respect to the ocean
406 surface area and a specific evaporation enthalpy of $L = 2\,501$ kJ kg^{-1}. At a surface humidity of $\psi_f =$
407 0.8, a value of $D_f(u) \approx 1.87 \times 10^{-4}$ kg m^{-2}s^{-1} can be concluded for the mass transfer coefficient,
408 and of $LD_f(u) \approx 468$ W m^{-2} for that of latent heat. Then, from

409 $$\Delta(LJ_W) = L \frac{\partial J_W}{\partial \psi_f} \Delta \psi_f = -LD_f(u) \frac{\Delta \psi_f}{\psi_f} \tag{13}$$

410 it follows that an increase by $\Delta \psi_f = 1$ %rh results in a heat flux reduction by $\Delta(LJ_W) =$
411 5.85 W m^{-2}. So, the currently observed ocean warming (Cheng et al. 2024) of 1.3 W m^{-2} could
412 theoretically be caused already by a minor marine humidity increase of $\Delta \psi_f = 0.2$ %rh, a value far
413 below the present measurement uncertainty between 1 and 5 %rh of relative humidity. The
414 resolution of climate models and observation seems to be insufficient yet to identify the possible role
415 of RH for the unclear explanation of the warming ocean.

416
417 **5 Sea Air as a Two-Phase Composite**

418 Gibbs' (1873) method of using potential functions can be applied to any systems possessing stable
419 thermodynamic equilibria and obeying energy conservation, without being restricted to merely
420 homogeneous or single-phase samples. The intentionally strict mutual consistency of the different
421 TEOS-10 potential functions permits a mathematical description of multi-phase composites such as
422 sea ice, consisting of ice with included brine pockets (Feistel and Hagen 1998, Feistel and Wagner
423 2005), or clouds, where liquid water or ice is floating in saturated humid air (Hellmuth et al. 2021).
424 Another important model is that of *sea air*, a sample consisting of a mass m^{SW} of seawater in
425 thermodynamic equilibrium with a mass m^{AV} of humid air (Feistel et al. 2010d, Feistel and Hellmuth
426 2023). Such a model may serve as a mathematical description for certain thermodynamic properties
427 of ocean-atmosphere interaction.

428 Extensive thermodynamic functions such as Gibbs energy or enthalpy are additive with respect to the
429 two separate phases of the sample. Equilibrium between those parts requires equal temperatures
430 and pressures. For this reason, a Gibbs function of sea air is an appropriate potential for the
431 composite system with $g^{SW}(S, T, p)$ describing the liquid part and $g^{AV}(A, T, p)$ the gas part. Let the
432 masses of the substances in the parts be m^W of liquid water, m^S of dissolved salt, m^A of dry air and
433 m^V of water vapour. Note that TEOS-10 neglects solubility of dry air constituents in liquid water.
434 From combinations of the partial masses follow the liquid mass, $m^{SW} = m^S + m^W$, the gas mass,
435 $m^{AV} = m^A + m^V$, the total mass $m = m^{SW} + m^{AV}$, the total water mass $m^{WV} = m^W + m^V$, the
436 salinity $S = m^S/m^{SW}$ and the dry-air fraction $A = 1 - q = m^A/m^{AV}$.

437 The Gibbs energies of the two phases of sea air are additive,

438 $$G^{SA} = G^{SW} + G^{AV} = mg^{SA}, \tag{14}$$

439 And, accordingly, the Gibbs function of sea air, g^{SA}, may be constructed from that of seawater,
440 $g^{SW}(S, T, p)$, with a liquid mass fraction of $w^{SW} = m^{SW}/m$ and that of humid air, $g^{AV}(A, T, p)$, with
441 a gaseous mass fraction of $w^{AV} = m^{AV}/m = 1 - w^{SW}$,

442 $$g^{SA}(S, A, w^{SW}, T, p) = w^{SW} g^{SW}(S, T, p) + (1 - w^{SW}) g^{AV}(A, T, p). \tag{15}$$

443 If the two phases are assumed to be at mutual equilibrium, they possess the same temperature,

444 pressure and chemical potentials, see eq. (B.11) in Appendix B, $\mu_W^{SW} = \mu_V^{AV}$, namely that of water in

445 seawater,

446 $\mu_W^{SW}(S, T, p) = g^{SW} - S \left(\frac{\partial g^{SW}}{\partial S} \right)_{T,p}$, (15)

447 equating that of water vapour in humid air,

448 $\mu_V^{AV}(A, T, p) = g^{AV} - A \left(\frac{\partial g^{AV}}{\partial A} \right)_{T,p}$. (16)

449

450 *5.1 Sea Air as a Model for Latent Heat of Evaporation*

451 Water evaporated from the ocean surface drives the climate system. "The by far largest part of heat

452 conveyed to the air is in the form of latent heat during subsequent condensation along with cloud

453 formation. The heat budget over the sea is mainly controlled by the latent heat released to the air"

454 (Albrecht 1940). It is the "*heat source for a gigantic steam engine*", as Heinrich Hertz had put it in his

455 1885 inaugural lecture at Karlsruhe (Mulligan and Hertz 1997). The latent heat of evaporation of pure

456 liquid water into pure water vapour is numerically well known from experiments (IAPWS SR1-86

457 1992, Harvey 1998, Wagner and Pruß 2002). Slightly differing values are reported in various

458 textbooks on hydrology (Debski 1966: p. 332), meteorology (Linke and Baur 1970) or geophysics (Gill

459 1982, Kraus and Businger 1994). TEOS-10, however, permits the computation of evaporation

460 properties from seawater into humid air, based on the first-time availability of standard equations

461 for enthalpies and chemical potentials of those non-ideal mixtures.
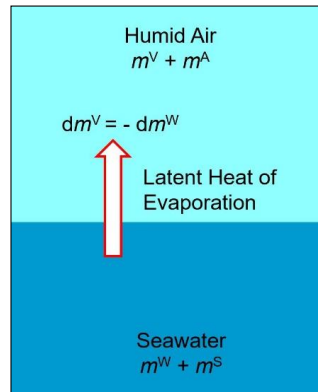
462

463 Fig. 8: Conceptual thermodynamic "sea air" model of ocean-atmosphere interaction as a two-phase

464 composite of seawater and humid air

465

466 If an infinitesimal amount of water is transferred from the liquid to the gas phase (Fig. 8), while

467 temperature and pressure remain at their equilibrium values, and the total masses of salt, m^S, dry

468 air, m^A, and water, m^{WV}, are not affected, the isobaric-isothermal latent heat of evaporation may be

469 defined by

470 $L^{SA} \equiv \left(\frac{\partial H^{SA}}{\partial m^V} \right)_{T,p,m^S,m^A,m^{WV}}$. (17)

471 This latent heat accounts for the loss of total heat of the sea-air sample associated with the loss of

472 liquid water and equal gain of water vapour,

473 $$\frac{\partial m^{\mathrm{V}}}{\partial T} = -\frac{\partial m^{\mathrm{W}}}{\partial T}.$$ (18)

474 Here, H^{SA} is the enthalpy of sea air, available from the Gibbs function (15) through the sum

475 $$H^{\mathrm{SA}} \equiv m^{\mathrm{SW}} h^{\mathrm{SW}} + m^{\mathrm{AV}} h^{\mathrm{AV}}.$$ (19)

476 Here, the specific enthalpies of seawater,

477 $$h^{\mathrm{SW}} = g^{\mathrm{SW}} - T \left(\frac{\partial g^{\mathrm{SW}}}{\partial T} \right)_{S,p},$$ (20)

478 and of humid air,

479 $$h^{\mathrm{AV}} = g^{\mathrm{AV}} - T \left(\frac{\partial g^{\mathrm{AV}}}{\partial T} \right)_{A,p},$$ (21)

480 are defined in terms of the related Gibbs functions.
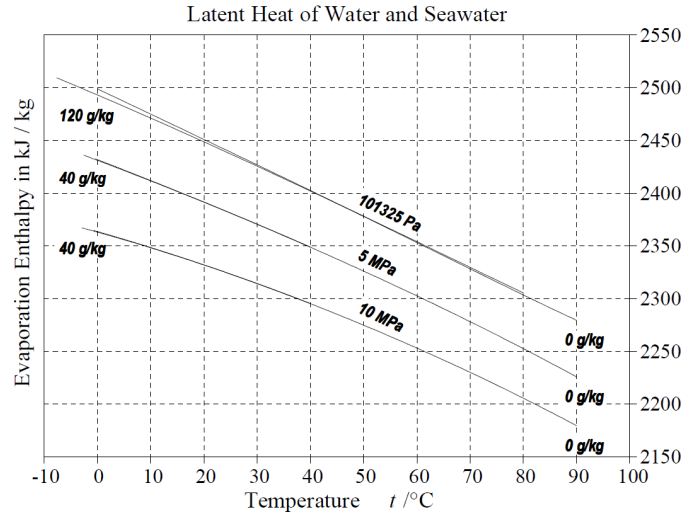
481

482 Fig. 9: Evaporation enthalpy, eq. (23), of seawater in equilibrium with humid air at different

483 temperatures, pressures and salinities. The dependence on salinity is very weak; graphically, the

484 related curves are hardly distinguishable. The nonlinear dependence on temperature is more

485 pronounced at elevated pressures. Figure from Feistel et al. (2010a: p. 105)

486

487 The derivative (17) is carried out in the form

488 $$L^{\mathrm{SA}} = -h^{\mathrm{SW}} - m^{\mathrm{SW}} \left(\frac{\partial h^{\mathrm{SW}}}{\partial S} \right)_{T,p} \left(\frac{\partial S}{\partial m^{\mathrm{V}}} \right)_{m^{\mathrm{S}}, m^{\mathrm{WV}}} + h^{\mathrm{AV}} + m^{\mathrm{AV}} \left(\frac{\partial h^{\mathrm{AV}}}{\partial A} \right)_{T,p} \left(\frac{\partial A}{\partial m^{\mathrm{V}}} \right)_{m^{\mathrm{A}}},$$ (22)

489 which results in the TEOS-10 latent-heat equation (Feistel et al. 2010a, Feistel and Hellmuth 2023),

490 $$L^{\mathrm{SA}} = h^{\mathrm{AV}} - A \left(\frac{\partial h^{\mathrm{AV}}}{\partial A} \right)_{T,p} - h^{\mathrm{SW}} + S \left(\frac{\partial h^{\mathrm{SW}}}{\partial S} \right)_{T,p},$$ (23)

491 with typical values shown in Fig. 9. If seawater is in mutual equilibrium with humid air at given
492 temperature and pressure, salinity and humidity of the parts of sea air satisfy the condition $\mu_W^{SW} = \mu_V^{AV}$, given by eqs. (15) and (16),
493

494 $$\Delta\mu \equiv g^{SW} - S\left(\frac{\partial g^{SW}}{\partial S}\right)_{T,p} - g^{AV} + A\left(\frac{\partial g^{AV}}{\partial A}\right)_{T,p} = 0 \qquad (24)$$

495 At given masses of salt, m^S, of dry air, m^A, and of total water, $m^{WV} = m^W + m^V$, eq. (24) controls
496 the value of either m^W or m^V, and this way also of S and A as functions of T, p, m^S, m^A and m^{WV}.
497 Related numerical solutions are readily implemented in the TEOS-10 SIA library; the latent heat of
498 sea air can be computed by calling the function sea_air_enthalpy_evap_si(), see Wright et al.
499 (2010).

500 Latent heat of eq. (23) is valid regardless of the equilibrium condition, eq. (24), is satisfied or not. The
501 non-equilibrium case is considered separately in Section 5.3.

502

503 *5.2 Sea Air as a Model of Sea Spray*

504 As a special form of air-sea interaction, sea spray is typically ejected from the crest of a breaking
505 wave, which may happen all along oceanic coasts but also wherever whitecaps are produced from
506 swell or stormy sea state, see Fig. 10. In contrast to fresh-water haze, droplets of sea spray cannot
507 completely evaporate for the salt they contain, and rather develop into a floating persistent Köhler
508 (1936) equilibrium between droplet size, droplet salinity and ambient relative fugacity. This
509 equilibrium can be described by the TEOS-10 model of sea air if the additional Kelvin pressure caused
510 by the surface tension is allowed for.

511

512 Fig. 10: Sea spray ejection from a breaking wave crest of Atlantic swell. Photo taken at Cabo Trafalgar
513 in March 2011.

514

515 In the infrared spectral range, sea spray as well as other aerosols (Carlon 1970, 1980) may be
516 considered as a black absorber and emitter of thermal radiation. The resulting "gray atmosphere" is a
517 conveniently simple conceptual model for the long-wave radiative effects of dust or haze in the

518 climate system (Emden 1913). When heated from below, as in the case of the clear-sky marine
519 troposphere, a theoretical finding is that the thermally stratified gray troposphere exhibits a special
520 critical value of the isobaric heat capacity at $c_p = 4R$ (Pierrehumbert 2010: p. 201), R being the
521 molar gas constant. Vertical stability may be lost at $c_p > 4R$ and turbulent mixing is expected to
522 commence (Feistel 2011: eq. 58 therein). Such a kinetic phase transition could substantially modify
523 the thermal radiation balance between troposphere and ocean surface.

524 The terrestrial atmosphere is dominated by the two-atomic gases N₂ and O₂ with heat capacities
525 about $3.5\,R$ which prevent the putative radiative vertical instability to occur. This situation may
526 change, however, in the presence of haze or sea spray. To investigate this effect theoretically, in this
527 section a TEOS-10 equation for the heat capacity of equilibrium sea air is derived from the definition

528
$$c_p^{\text{SA}} \equiv \frac{1}{m}\left(\frac{\partial H^{\text{SA}}}{\partial T}\right)_{p,m^{\text{S}},m^{\text{A}},m^{\text{WV}}}.$$
(25)

529 The enthalpy of sea air is given by eq. (19). Taking into account water conservation upon
530 evaporation, $m^{\text{WV}} = \text{const}$, that is,

531
$$\frac{\partial m^{\text{V}}}{\partial T} = -\frac{\partial m^{\text{W}}}{\partial T},$$
(26)

532 and of eq. (23), the isobaric heat capacity of sea air is concluded to be

533
$$c_p^{\text{SA}} = w^{\text{SW}} c_p^{\text{SW}} + w^{\text{AV}} c_p^{\text{AV}} + L^{\text{SA}} \frac{1}{m}\frac{\partial m^{\text{V}}}{\partial T}.$$
(27)

534 To the additive contributions of the partial heat capacities of the liquid and the gas part, there
535 appears the latent heat of the water mass that evaporates from the liquid as vapour. This
536 evaporation rate is governed by the mutual equilibrium between seawater and humid air.

537 During the temperature change, sea-air equilibrium, eq. (24), is assumed to be maintained by water
538 transfer between the phases, changing S and A along with T,

539
$$\left(\frac{\partial \Delta \mu}{\partial T}\right)_{p,m^{\text{S}},m^{\text{A}},m^{\text{WV}}} = 0.$$
(28)

540 Carrying out the derivative, this condition reads

541
$$\left(\frac{\partial g^{\text{SW}}}{\partial T}\right)_{S,p} - S\left(\frac{\partial^2 g^{\text{SW}}}{\partial S \partial T}\right)_p - S\left(\frac{\partial^2 g^{\text{SW}}}{\partial S^2}\right)_{T,p}\left(\frac{\partial S}{\partial T}\right)_{m^{\text{S}}}$$

542
$$= \left(\frac{\partial g^{\text{AV}}}{\partial T}\right)_{A,p} - A\left(\frac{\partial^2 g^{\text{AV}}}{\partial A \partial T}\right)_p - A\left(\frac{\partial^2 g^{\text{AV}}}{\partial A^2}\right)_{T,p}\left(\frac{\partial A}{\partial T}\right)_{m^{\text{A}}}.$$
(29)

543 On the other hand, from combining eq. (23) with eq. (24) it follows that the latent heat may be
544 expressed by,

545
$$L^{\text{SA}} = T\left\{\left(\frac{\partial g^{\text{SW}}}{\partial T}\right)_{S,p} - S\left(\frac{\partial^2 g^{\text{SW}}}{\partial S \partial T}\right)_p - \left(\frac{\partial g^{\text{AV}}}{\partial T}\right)_{A,p} + A\left(\frac{\partial^2 g^{\text{AV}}}{\partial A \partial T}\right)_p\right\},$$
(30)

546 so that eq. (29) may be written as

547
$$L^{\text{SA}} = T\left\{S\left(\frac{\partial^2 g^{\text{SW}}}{\partial S^2}\right)_{T,p}\left(\frac{\partial S}{\partial T}\right)_{m^{\text{S}}} - A\left(\frac{\partial^2 g^{\text{AV}}}{\partial A^2}\right)_{T,p}\left(\frac{\partial A}{\partial T}\right)_{m^{\text{A}}}\right\}.$$
(31)

548 Further, the total water mass balance, eq. (26), implies that

549
$$\left(\frac{\partial S}{\partial T}\right)_{m^{\text{S}}} = \left(\frac{\partial S}{\partial m^{\text{W}}}\right)_{m^{\text{S}}}\frac{\partial m^{\text{W}}}{\partial T} = \frac{S}{m^{\text{SW}}}\frac{\partial m^{\text{V}}}{\partial T},$$
(32)

550 and similarly,

551
$$\left(\frac{\partial A}{\partial T}\right)_{m^A} = \left(\frac{\partial A}{\partial m^V}\right)_{m^A} \frac{\partial m^V}{\partial T} = -\frac{A}{m^{AV}} \frac{\partial m^V}{\partial T}. \quad (33)$$

552 Inserting those expressions into eq. (31), the equation for the isobaric evaporation rate of sea air is

553
$$\frac{\partial m^V}{\partial T} = \frac{L^{evap}}{T} \left\{ \frac{S^2}{m^{SW}} \left(\frac{\partial^2 g^{SW}}{\partial S^2}\right)_{T,p} + \frac{A^2}{m^{AV}} \left(\frac{\partial^2 g^{AV}}{\partial A^2}\right)_{T,p} \right\}^{-1}. \quad (34)$$

554 Together with eq. (34), the desired formula for the isobaric heat capacity (27) of sea air finally
555 becomes (Feistel et al. 2010a: eq. 6.22 therein),

556
$$c_p^{SA} = w^{SW} c_p^{SW} + \left(1 - w^{SW}\right) c_p^{AV} + \frac{\left(L^{SA}\right)^2}{T} \left\{ \frac{S^2}{w^{SW}} \left(\frac{\partial^2 g^{SW}}{\partial S^2}\right)_{T,p} + \frac{A^2}{(1-w^{SW})} \left(\frac{\partial^2 g^{AV}}{\partial A^2}\right)_{T,p} \right\}^{-1}. \quad (35)$$

557 Of the *liquid water content*, expressed in form of the liquid mass fraction, w^{SW}, realistic values may
558 typically range between 10^{-6} and 10^{-4} in the troposphere. Growing along with this fraction, related
559 heat capacities of sea air, eq. (35), may substantially exceed that of liquid-free humid air, c_p^{AV}, see
560 Fig. 11.
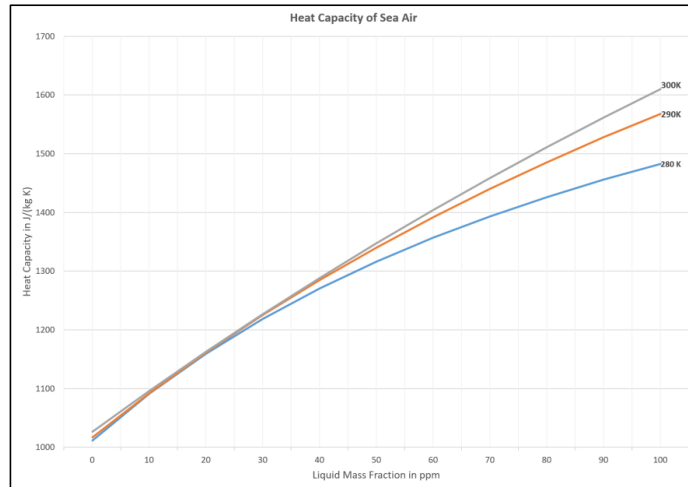
561

562 Fig. 11: TEOS-10 values for the isobaric specific heat capacity, eq. (35), of sea air at atmospheric
563 pressure and sea-spray standard-ocean salinity, S = 35.165 04 g kg⁻¹, at temperatures of 280 K (lower
564 curve), 290 K (middle curve) and 300 K (upper curve) as functions of the liquid mass fraction, w^{SW},
565 up to 100 ppm.

566

567 *5.3 Sea Air as a Model for Irreversible Evaporation*

568 The climate system functions far from thermodynamic equilibrium, permanently producing and
569 exporting entropy at an average rate of 1 W m⁻² K⁻¹ per global surface area (Ebeling and Feistel 1982,
570 Feistel and Ebeling 2011). By contrast, TEOS-10 is a mathematical description of equilibrium
571 properties (Appendix B). The latter is applicable to states away from thermodynamic equilibrium
572 under the assumption of *local equilibrium* as introduced by Ilya Prigogine (1947, 1978). This
573 assumption means that spatially extended substances such as ocean or atmosphere consist of
574 sufficiently small volume elements that may reasonably be described as macroscopic equilibrium

575   states, homogeneous in temperature, pressure and chemical potentials. TEOS-10 thermodynamic
576   potentials can be used to describe those local states.

577   By definition, if a volume at equilibrium is divided into partial volumes, each of those parts is at
578   equilibrium itself, and each pair of those is at mutual equilibrium also. The combination of several
579   local-equilibrium elements forms a non-equilibrium state if pairs of elements exist that are out of
580   mutual equilibrium. Extensive properties such as mass, energy, entropy or enthalpy can be added up
581   to give correct values of the entire system. When exchange processes between those elements
582   occur, gains and losses of masses, energies or enthalpies are mutually balanced by conservation laws,
583   however, this is not the case for entropy.

584   A tutorial case of a local equilibrium system may be the model of sea air (Feistel and Hellmuth 2024a)
585   depicted in Fig. 8. It consists of a mass $m^{SW} = m^S + m^W$ of seawater in contact with a mass $m^{AV} =$
586   $m^A + m^A$ of humid air. Both fluids are assumed to be at internal equilibrium themselves but not
587   necessarily in mutual equilibrium with one another. This is a natural geophysical situation – marine
588   RH has typical values of 80 %rh while the equilibrium of humid air with seawater, eq. (24), is
589   established at about 98 %rh. For simplicity, let all parts have equal temperatures and pressures.

590   If evaporation takes place, the partial water masses involved will change by a mass flux across the
591   sea surface,

592
$$J_m \equiv \frac{\mathrm{d}m^{AV}}{\mathrm{d}t} = \frac{\mathrm{d}m^V}{\mathrm{d}t} = -\frac{\mathrm{d}m^{SW}}{\mathrm{d}t} = -\frac{\mathrm{d}m^W}{\mathrm{d}t}. \tag{36}$$

593   The change of the total enthalpy of the sea-air sample is available from eqs. (17) and (23),

594
$$\frac{\mathrm{d}H^{SA}}{\mathrm{d}t} = \left(\frac{\partial H^{SA}}{\partial m^V}\right)_{T,p,m^S,m^A,m^{WV}} \frac{\mathrm{d}m^V}{\mathrm{d}t} = L^{SA} J_m . \tag{37}$$

595   This expression of energy conservation, the 1st law of thermodynamics, is similarly valid for
596   equilibrium and non-equilibrium conditions of the sample. For comparison, of the total entropy
597   defined by,

598
$$N^{SA} \equiv m^{SW}\eta^{SW} + m^{AV}\eta^{AV}, \tag{38}$$

599   the change is given by

600
$$\frac{\mathrm{d}N^{SA}}{\mathrm{d}t} = \left(\frac{\partial N^{SA}}{\partial m^V}\right)_{T,p,m^S,m^A,m^{WV}} \frac{\mathrm{d}m^V}{\mathrm{d}t} . \tag{39}$$

601   In terms of its two parts, eq. (38), this change takes the form,

602
$$\frac{\mathrm{d}N^{SA}}{\mathrm{d}t} = \left[\eta^{AV} - A\left(\frac{\partial \eta^{AV}}{\partial A}\right)_{T,p} - \eta^{SW} + S\left(\frac{\partial \eta^{SW}}{\partial S}\right)_{T,p}\right] J_m. \tag{40}$$

603   Making use of their local equilibria, specific entropy of each part can be expressed by the difference,
604   eq. (B.6),

605
$$\eta = \frac{h-g}{T}, \tag{41}$$

606   between specific enthalpy, h, and specific Gibbs energy, g, so that the entropy change becomes

607
$$T\frac{\mathrm{d}N^{SA}}{\mathrm{d}t} = \left(L^{SA} + \Delta\mu\right)J_m. \tag{42}$$

608   Here, the latent heat, L^{SA}, is given by eq. (23), and the distance from mutual equilibrium, $\Delta\mu$, by eq.
609   (24).

610   The first term,

611    $T\frac{\mathrm{d}_e N^{\mathrm{SA}}}{\mathrm{d}t} \equiv L^{\mathrm{SA}} J_m,$
(43)

612   is the *external* entropy change (subscript e) in the form of the heat flux required to maintain the
613   sample's temperature, compensating the storage of latent heat by emitting water vapour.

614   The second term,

615    $T\frac{\mathrm{d}_i N^{\mathrm{SA}}}{\mathrm{d}t} \equiv J_m \Delta\mu.$
(44)

616   is the *internal* entropy change (subscript i), or *entropy production*, of the non-equilibrium sea-air
617   sample. It represents the additional entropy gain of humid air compared to the entropy loss of
618   seawater. This production happens at the air-sea interface and disappears as soon as mutual
619   equilibrium, $\Delta\mu = 0$, is approached.

620   It is important to be aware that the external part, $\frac{\mathrm{d}_e N^{\mathrm{SA}}}{\mathrm{d}t}$, *always* constitutes a contribution to the
621   system's energy balance while, by contrast, the internal part, $\frac{\mathrm{d}_i N^{\mathrm{SA}}}{\mathrm{d}t}$, is *never* any such contribution.
622   The irreversible production of entropy is an internal conversion or redistribution of energy rather
623   than a change of it. This implies that irreversible processes violate Gibbs' fundamental equation (B.8)
624   in the sense that

625    $\frac{\mathrm{d}H^{\mathrm{SA}}}{\mathrm{d}t} = -T\frac{\mathrm{d}_e N^{\mathrm{SA}}}{\mathrm{d}t} + V^{\mathrm{SA}}\frac{\mathrm{d}p}{\mathrm{d}t} + \sum_i \mu_i \frac{\mathrm{d}m_i}{\mathrm{d}t} > -T\frac{\mathrm{d}N^{\mathrm{SA}}}{\mathrm{d}t} + V^{\mathrm{SA}}\frac{\mathrm{d}p}{\mathrm{d}t} + \sum_i \mu_i \frac{\mathrm{d}m_i}{\mathrm{d}t},$
(45)

626   even though each of its local-equilibrium elements strictly satisfies the related fundamental equation
627   (B.13), valid for reversible processes only,

628    $dh = -Td\eta + vdp + \sum_{i=1}^{n-1}(\mu_i - \mu_0)\mathrm{d}w_i.$
(46)

629   Entropy production appears wherever a flux is passing its driving gradient. Near equilibrium, this flux
630   is proportional to its driving force (Glansdorff and Prigogine 1971, Landau and Lifschitz 1974, Kraus
631   and Businger 1994, Feistel and Hellmuth 2024a), usually termed *Onsager force*. For example, the
632   evaporation mass flux of water, eq. (6),

633    $J_m = C\,\Delta\mu$
(47)

634   may be assumed as being proportional to the difference between the chemical potentials of water
635   across the air-sea interface. The related *Dalton equation* (6) was discussed in Section 4. The
636   associated entropy production, eq. (44), obeys the 2nd law of thermodynamics by the inequality

637    $\frac{\mathrm{d}_i N^{\mathrm{SA}}}{\mathrm{d}t} = C\,(\Delta\mu)^2 \geq 0,$
(48)

638   while the total entropy change, eq. (42) may possess any sign. In other words, the 2nd law forbids that
639   *Onsager fluxes* may be directed against their causing Onsager forces.

640   Processes accompanied by entropy production are termed *irreversible* ones, since entropy once
641   created may never be destroyed again. Related processes cannot be reversed unless lasting changes
642   are left behind in the external world. By contrast, processes which transform an equilibrium state
643   into another equilibrium state may *reversibly* be performed without producing entropy. Entropy
644   production is possible only under non-equilibrium conditions.

645   Under typical marine circumstances, the entropy production density of ocean evaporation can be
646   estimated to about 4 mW K^{-1} m^{-2}, contributing roughly 0.4 % to the global entropy production
647   (Feistel and Ebeling 2011, Feistel and Hellmuth 2024a).

648

649   **6   Cloudiness and Ocean Warming**

650   On the long-term average, cloudiness is particularly strong in the low-pressure belts of the global
651   tropospheric circulation, where air is ascending and its humidity is condensing, see Fig. 12. Except for
652   the equatorial zone, those spatial cloudiness pattern correlate visibly with those of recent ocean
653   warming, compare Fig. 1. It is a plausible working hypothesis that this correlation could also indicate
654   a causal relation between the two phenomena. However, such correlations imply hen-and-egg
655   problems (Rapp 2014): putative causality relations between those trends cannot be derived from
656   observation but only be concluded from reliable prediction models (Feistel 2023). May the observed
657   systematic reduction of global cloudiness (Fasullo and Trenberth 2012) actually be responsible for
658   the currently recorded excessive ocean warming (You 2024)? Unfortunately, and somewhat
659   surprisingly, this assumption can apparently not be underpinned yet by closer investigation. Some
660   related issues will be discussed in this section.
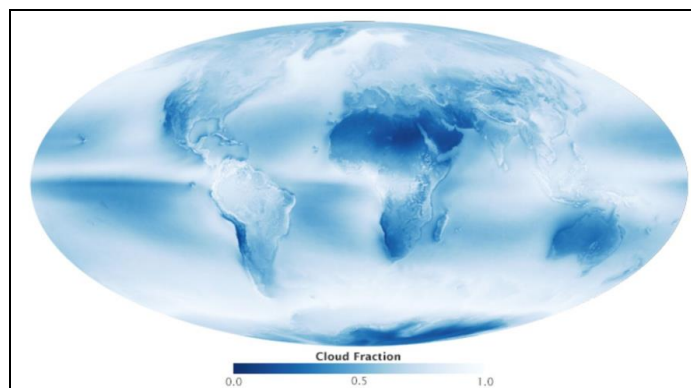
661

662   Fig. 12: Global distribution of cloudiness July 2002 – April 2015 (Allen and Ward 2015). Image
663   reproduction permitted by NASA Copyright.

664   *6.1 Cloudiness Trend*

665   Global cloud-covered surface area fraction C has systematically been reducing by about 6 % per
666   century, see Fig. 13, from $C \approx 67.5$ % in 1980 to $C \approx 65$ % in 2022 (Foster et al. 2023, Phillips and
667   Foster 2023). Observed cloudiness values depend strongly on the way clouds are defined (Spänkuch
668   et al. 2022) and on the measurement technology applied. For example, Rapp (2014: Fig. 6.20)
669   reported a decrease in cloudiness in 30 years from 70 % in 1983 down to 63.5 % in, likely, 2013. This
670   reduction rate of more than 20 % per century is three times as fast as that given in Fig. 13 and may
671   result from different observation techniques.
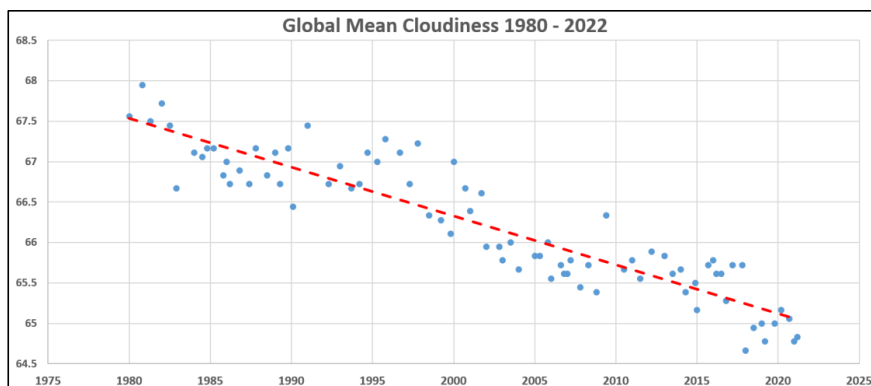
672

673 Fig. 13: Dots: satellite-derived global mean cloud area fractions 1980-2022 in percent. Data from
674 Foster et al. (2023). Dashed line: present cloudiness is 65 % with a climatological linear shrinking
675 trend of −6.2 % per century.

676

677 Assuming that this shrinking occurred in a similar way above both land and sea, the ocean is
678 expected to receive increasingly more solar irradiation. This phenomenon is known as the *short-wave*
679 *cloud radiative effect* (SW CRE), see Fig. 14.
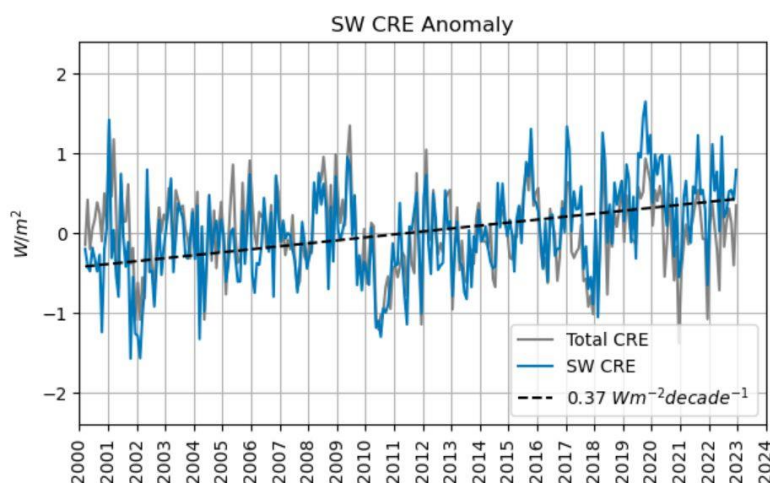
680

681 Fig. 14: Short-wave cloud radiative effect (SW CRE) of increasing solar irradiation. Image kindly
682 provided by Coda Phillips (priv. comm.), with minor correction compared to the original publication
683 (Phillips and Foster 2023). Total CRE is the net effect of SW and LW CRE, see Fig. 15.

684

685 On the other hand, clouds are opaque with respect to oceanic upward thermal radiation and emit
686 themselves downward infrared radiation. This phenomenon is known as the *long-wave cloud*
687 *radiative effect* (LW CRE), see Fig. 15. Radiation models show that on the global average these two
688 effects cancel each other almost completely up to minor rest of −1 mW m^{-2} yr^{-1}, so that the
689 continuously shrinking cloudiness may be assumed to have practically no net effect on the ocean's
690 radiation balance (Phillips and Foster 2023, Feistel and Hellmuth 2024b). However, more detailed

691   investigations in the future may reveal more rigorous results for the ocean than this simplified

692   picture.
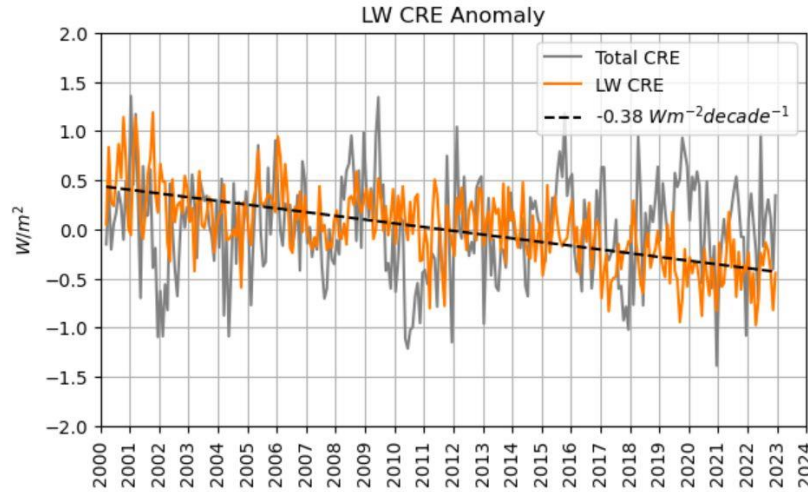
693

694   Fig. 15: Long-wave cloud radiative effect (LW CRE) of decreasing net thermal radiation. Image kindly

695   provided by Coda Phillips (priv. comm.), with minor correction compared to the original publication

696   (Phillips and Foster 2023). Total CRE is the net effect of SW and LW CRE, see Fig. 14.

697

698   *6.1 Cumulus Clouds*

699   Cumulus clouds are often formed in the course of diurnal convection by isentropic uplift of humid air

700   parcels from the sea surface to the condensation level, mostly located at low heights between 200

701   and 500 m. This process permits a thermodynamic description of such clouds (Romps 2014) by

702   calculating the *lifted condensation level* (LCL) as the cumulus cloud base. As the first such

703   international geophysical standard, TEOS-10 provides explicit equations for entropy, enthalpy and

704   chemical potentials of humid air which may be used to derive reference equations and values of the

705   LCL (Feistel and Hellmuth 2024b).

706   At the sea surface pressure, p_0, the air parcel may possess the temperature T_0 and the relative

707   fugacity ψ_f, which is a real-gas definition of relative humidity (Feistel and Lovell-Smith 2017) in terms

708   of the chemical potential of water vapour in humid air, μ_V^{AV}, and that of liquid water, μ_W,

709    $$R_W T_0 \ln \psi_f = \mu_V^{AV}(A, T_0, p_0) - \mu_W(T_0, p_0). \tag{49}$$

710   Here, $R_W = 461.523 \text{ J kg}^{-1} \text{ K}^{-1}$ is the specific gas constant of water, and $A = 1 - q$ is the dry-air

711   mass fraction of the parcel, to be determined from ψ_f by this condition.

712   At the LCL, the parcel is saturated at $\psi_f = 1$, i.e.,

713    $$0 = \mu_V^{AV}(A, T_{LCL}, p_{LCL}) - \mu_W(T_{LCL}, p_{LCL}). \tag{50}$$

714   During uplift, A is assumed to remain constant, as well as the parcel's entropy, η^{AV},

715    $$\eta^{AV}(A, T_0, p_0) = \eta^{AV}(A, T_{LCL}, p_{LCL}). \tag{51}$$

716
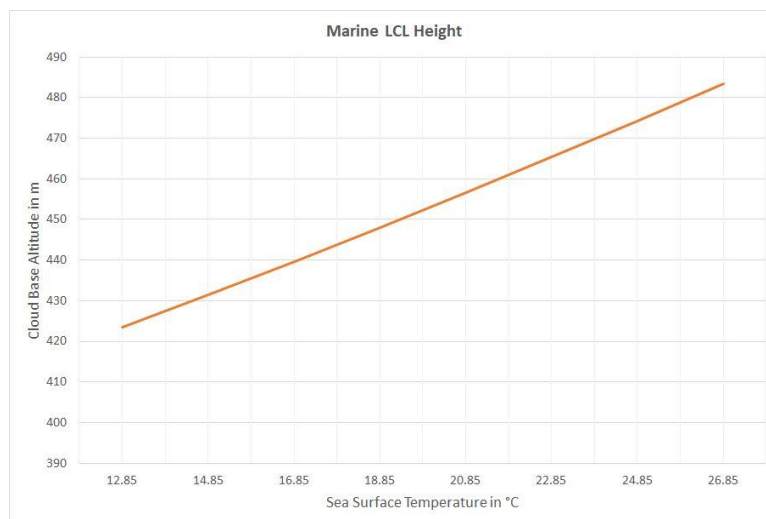
717
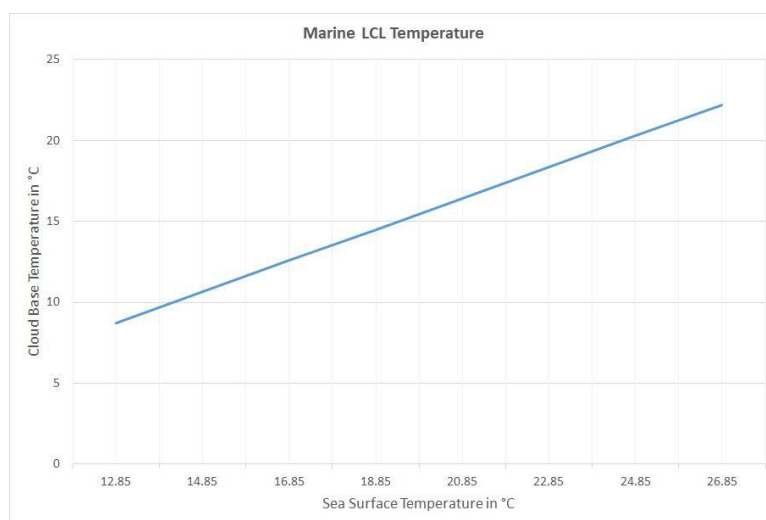
718

719 Fig. 16: As a function of typical low-latitude sea-surface temperatures, LCL height (top) and LCL
720 temperature (bottom) are computed from the TEOS-10 equations (49) – (52) at a typical marine
721 surface RH of 80 %rh.

722

723 Finally, the LCL altitude, z_{LCL}, above sea level follows from the isentropic integral of the hydrostatic
724 equation in terms of the enthalpy, h^{AV}, of humid air,

725 $$z_{\text{LCL}} = \frac{1}{g_{\text{E}}}\left[h^{\text{AV}}(A, \eta^{\text{AV}}, p_0) - h^{\text{AV}}(A, \eta^{\text{AV}}, p_{\text{LCL}})\right].$$ (52)

726 The gravity acceleration is $g_{\text{E}} = 9.81 \text{ m s}^{-2}$. The functions μ_V^{AV}, η^{AV}, h^{AV} and μ_W can be expressed
727 by partial derivatives of the TEOS-10 thermodynamic potentials of humid air and liquid water, and
728 are numerically available from the *Sea-Ice-Air* (SIA) *library* (Feistel et al. 2010d, Wright et al. 2010).

729 Solving eqs. (49) – (52) numerically, the LCL properties $(A, T_{\text{LCL}}, p_{\text{LCL}}, z_{\text{LCL}})$ are obtained from the
730 given surface properties, (ψ_f, T_0, p_0).

731 As solutions of eqs. (49) – (52), height and base temperature of marine cumulus clouds, as a function
732 of the sea-surface temperature T_0 at a sea-surface relative fugacity of $\psi_f = 80$ %rh, are displayed in
733 Fig. 16. Similarly, height and base temperature, as a function of the sea-surface relative fugacity of
734 ψ_f at a sea-surface temperature $T_0 = 292$ K, close to the current global mean SST, are displayed in
735 Fig. 17.
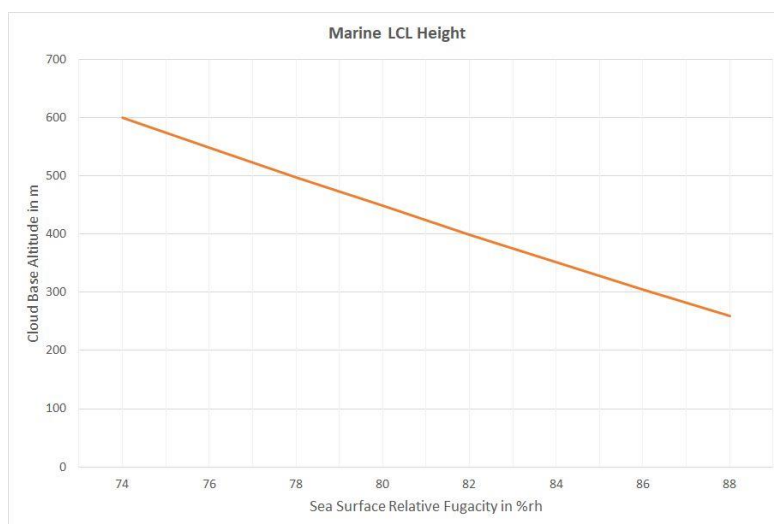
736
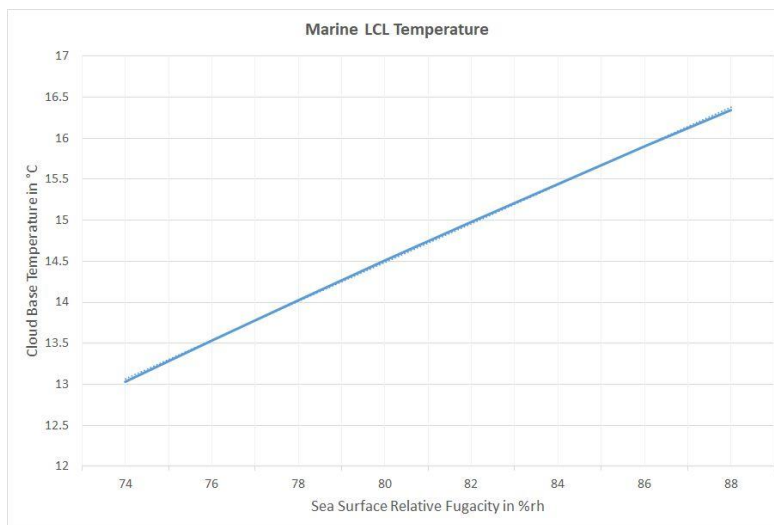
737

738 Fig. 17: As a function of typical marine RH values, LCL height (top) and LCL temperature (bottom) are
739 computed from the TEOS-10 equations (49) – (52) at a sea surface temperature of 292 K, close to the
740 current global mean SST of 18.8 °C, see Fig. 18.

741

742

743 Table 1: LCL cloud-base temperatures, T_{LCL}, pressures, p_{LCL}, and heights, z_{LCL}, as functions of the
744 SST, T_0, at marine surface relative fugacity of $\psi_f = 80$ %rh, computed from TEOS-10 eqs. (49) – (52),
745 as well as climatic LCL sensitivities, α, β, γ, eq. (53), with respect to increasing SST (Feistel and
746 Hellmuth 2024). The row printed in bold approximates the current global mean SST, see Fig. 18.

T_0 K	T_{LCL} K	p_{LCL} hPa	z_{LCL} m	α % K^{-1}	β K K^{-1}	γ hPa K^{-1}
286	281.883	963.093	423.468	−0.0483	0.9634	−0.2742
288	283.810	962.542	431.481	−0.0542	0.9629	−0.2773
290	285.735	961.984	439.660	−0.0608	0.9624	−0.2806
292	**287.659**	**961.419**	**448.017**	**−0.0680**	**0.9619**	**−0.2841**
294	289.583	960.847	456.561	−0.0759	0.9614	−0.2878
296	291.505	960.268	465.305	−0.0846	0.9608	−0.2917
298	293.426	959.680	474.263	−0.0942	0.9603	−0.2959
300	295.346	959.084	483.449	−0.1047	0.9597	−0.3004

747

748
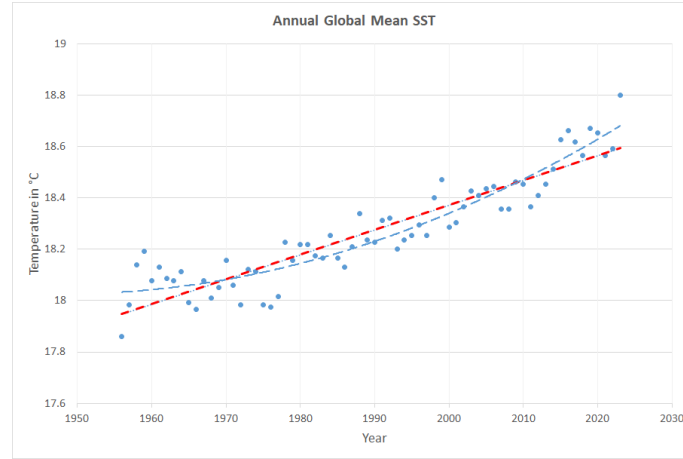
749

750 Fig. 18: Estimated increase 1957 – 2023 of global annual mean sea-surface temperatures (source:
751 Cheng et al. 2024). The linear trend (red) is $t/°C \approx 18 + 0.01 \times (yr - 1961)$. The quadratic trend
752 curve (blue) suggests an acceleration of warming.

753

754 Global mean sea-surface temperature has risen from about 17.9 °C in 1956 to 18.8 °C in 2023 (Cheng
755 et al. 2024), see Fig. 18. This pronounced climatic trend is expected to let the cumulus cloud base lift
756 up while at the same time warming it, see Fig. 16, but less than the SST itself is increasing. The
757 related climatic sensitivities possess complicated dependencies but may directly be derived by taking
758 the related derivatives

759 $\alpha \equiv \left(\frac{\partial A}{\partial T_0} \right)_{p_0, \psi_f} = - \left(\frac{\partial q}{\partial T_0} \right)_{p_0, \psi_f}, \beta \equiv \left(\frac{\partial T_{\text{LCL}}}{\partial T_0} \right)_{p_0, \psi_f}$ and $\gamma \equiv \left(\frac{\partial p_{\text{LCL}}}{\partial T_0} \right)_{p_0, \psi_f},$ (53)

760 of the TEOS-10 LCL equations (49) – (52) with respect to the surface temperature while keeping
761 surface RH fixed (Feistel and Hellmuth 2024). Selected results for those sensitivities are given in Table
762 1 relative to 1 °C rise of SST, similar to that in the past 70 years (Fig. 16). Here, $\alpha \approx -0.07$ % K^{-1}

763   describes the rate of increase of specific humidity at the sea surface, often dubbed the "Clausius-

764   Clapeyron effect". The value of $\beta \approx 0.96$ indicates that the cumulus cloud base warms up slower

765   that the ocean by about 4 %, and $\gamma \approx -0.28$ hPa K^{-1} is the LCL pressure lowering caused by ocean

766   warming, corresponding to ascending clouds. The value $\beta < 1$ implies that the thermal downward

767   radiation from the cloud base does not keep pace with the ocean upward radiation, so that the net

768   climatic feedback of cumulus clouds is negative and acts against ocean warming. These clouds do not

769   provide a physical explanation for the observed enhanced ocean warming.

770

771   *6.2 Stratocumulus and Other Clouds*

772   The dominating cloud type over the ocean is stratocumulus (Eastman et al. 2011). "They are common

773   over the cooler regions of subtropical and midlatitude oceans where their coverage can exceed 50%

774   in the annual mean" (Wood 2012: p. 2373) with a typical thickness about 320 m and "a tendency for

775   thicker clouds (median 420 m) in mid- and high latitudes" (Wood 2012: p. 2378). "Stratocumuli tend

776   to form under statically stable lower-tropospheric conditions" (Wood 2012: p. 2374). On the annual

777   average, stratocumulus is particularly frequent (up to 60 % coverage) at the subtropical coastal

778   upwelling regions such as the cold Benguela, Humboldt and California Currents (Wood 2012: Fig. 4a,

779   Muhlbauer et al. 2014: Fig. 2). However, in those areas there is no obvious correlation of cloud cover

780   with ocean warming (Fig. 1). Stratocumulus also forms large cloud cover (about 20 % coverage) in the

781   boreal and austral west-wind bands (Wood 2012: Fig. 4a) where the ocean is strongly warming up

782   (Fig. 1).

783   "Only small changes in the coverage and thickness of stratocumulus clouds are required to produce a

784   radiative effect comparable to those associated with increasing greenhouse gases" (Wood 2012: p.

785   2374). "Low-cloud feedbacks are also a leading cause of uncertainty in future climate prediction

786   because even small changes in cloud coverage and thickness have a major impact on the radiation

787   budget" (Wood 2012: p. 2373). Marine stratocumulus cloud feedback is still a major challenge and

788   source of uncertainty of climate models (Hirota et al. 2021). However, "similar to other low-cloud

789   types in the marine boundary layer, the impact of stratocumulus clouds on the outgoing longwave

790   radiation is marginal due to the lack of contrast between the temperature of stratocumulus cloud

791   tops and the temperature of the sea surface over which they form. Thus, the net radiative effect of

792   stratocumulus clouds is primarily controlled by factors influencing their shortwave cloud forcing such

793   as the cloud albedo and the cloud coverage" (Muhlbauer et al. 2014: p. 6695).

794   Following this argumentation and assuming that the short-wave cloud effect of stratocumuli on the

795   ocean radiation balance by far outweighs their long-wave effects, then the short-wave warming

796   effect (Fig. 14) of decreasing cloudiness may dominate over the long-wave cooling (Fig. 15). Possibly,

797   this could make stratocumulus a potential candidate for causing the unclear recent ocean warming.

798   Similarly, in the diurnal cycle, short wave effects (Fig. 14) have an impact at daytime only, while long

799   wave effects (Fig. 15) are present all 24 hours. Regionally, where in spring the days get longer, and

800   the heavy cloudiness of the west-wind belt becomes replaced by fewer subtropical clouds (see Fig.

801   12), the systematic reduction of cloudiness may be expected to produce local excess warming such as

802   near the subtropical fronts (see Fig. 1). Only dedicated future model studies, however, may reliably

803   verify such speculations.

804

805

806

807 7   Summary

808   Substantial uncertainties of estimated heat fluxes at the ocean-atmosphere interface, such as the
809   "ocean heat budget closure problem", prevent reliable model predictions and causal explanations of
810   climate phenomena that may take place within the range of those uncertainties. Among such
811   "surprises" is the currently registered excessive ocean warming, but are, expectedly, also the
812   subsequent consequences of this warming for global weather processes.

813   Intending to reduce model uncertainties of thermal energies and heat fluxes in the climate system
814   associated with the global circulation of water in its different phases and mixtures, the new
815   geophysical thermodynamic standard TEOS-10 had been adopted internationally in 2009 and 2011.
816   Meanwhile, the uptake of TEOS-10 by the scientific community is mainly focussed on ocean
817   modelling, as the related publication metrics are suggesting (Appendix A).

818   TEOS-10 is advanced over previous similar standards and various collections of tailored empirical
819   property equations by (i) its completeness in describing all thermodynamic properties of seawater,
820   humid air and ice, including their entropies, enthalpies and chemical potentials, (ii) its perfect mutual
821   consistency between different phases and mixtures, and (iii) its minimum uncertainty over maximum
822   ranges of validity. Among its particularly favourable fields of application are composite systems with
823   internal phase boundaries such as air sea interaction or cloud formation.

824   In addition to entropies, enthalpies and chemical potentials, TEOS-10 has made available certain new
825   quantities for the description and modelling of climate processes, such as (i) Absolute Salinity of the
826   ocean with a specified Reference Composition, (ii) Conservative Temperature as a measure of
827   Potential Enthalpy of seawater representing a definite heat content, and (iii) Relative Fugacity as the
828   thermodynamic driving force of evaporation, suggesting an improved full-range definition of relative
829   humidity as a substitute for mutually inconsistent and restricted such definitions in practical use in
830   climatology, meteorology and physical chemistry.

831   This paper explains some tutorial examples for the application of TEOS-10 to selected current climate
832   problems. There is (i) the two-phase conceptual model of "sea air" which provides rigorous equations
833   for the latent heat of evaporation, for the heat capacity of humid air including salty aerosols (sea
834   spray), and for the irreversible production of entropy by evaporation into the marine troposphere.
835   There is also (ii) the formation of low marine cumulus clouds by isentropic thermal convection up to
836   their condensation level, and their climatic feedback to surface temperature and humidity
837   concerning their infrared radiation effects.

838   It is currently unclear why and how the ocean warming is intensifying, and when and how the related
839   enormous amount of heat may transfer to the atmosphere. The observed systematic reduction of
840   cloudiness may play an important role in this process, but responsible details and theoretical causes
841   are unknown. Marine surface relative humidity is an important and rather sensitive "control valve"
842   for the supply of the troposphere with latent heat, however, the common assumption of constant
843   relative humidity during climate change lacks rigorous explanation and leaves open the question of
844   its possible trends below the insufficiently high level of observational uncertainty. TEOS-10 may
845   further assist climate modellers to address such issues.

846   Ocean Science has proved a scientifically well-respected, reliable and successful partner journal for
847   the publication of advanced results and methods in oceanography and geophysics. Cooperation with
848   international bodies such as IUGG, UNESCO/IOC, IAPSO, SCOR, IAPWS and BIPM has made the
849   development and international introduction of TEOS-10 possible. The established standing
850   committee JCS remains active with respect to related fundamental problems still to be solved. It is

851 hoped and expected that TEOS-10 may constitute a reliable long-term thermodynamic basis for
852 interdisciplinary climate research.

853

854 **Appendix A: Summary and Metrics of Selected Publications Related to TEOS-10**

855 Between December 2008 and December 2012, supporting the activities of SCOR/IAPSO WG127,
856 *Ocean Science* had published 16 articles open-access in its Special Issue #14, "Thermophysical
857 properties of seawater" (Feistel et al. 2008). From February 2013 on, monthly metrics have been
858 recorded by the journal. Table A1 reports those metrics of the last decade.

859 For comparison, metrics – as far as published elsewhere by 04 April 2024 – of selected TEOS-10
860 articles listed at www.teos-10.org are reported in Table A2.

861 **Table A1**: Metrics of articles in the *Ocean Science* Special Issue #14, "Thermophysical properties of
862 seawater" (Feistel et al. 2008a), from February 2013 till March 2024. "SIA" stands for the TEOS-10
863 Sea-Ice-Air open source code library.

Reference	Topic	Accessed	PDF Downloads	Cited
Millero and Huang (2009)	Seawater at High T,S	16 462	11 061	79
Feistel et al. (2010c)	Baltic Sea Density/Salinity	15 435	11 385	92
Pawlowicz et al. (2011)	Seawater Biogeochemistry	9 663	6 444	47
McDougall et al. (2012)	Global Absolute Salinity	9 290	5 489	116
Feistel et al. (2010a)	Humid Air Helmholtz Function	8 737	5 346	31
Safarov et al. (2009)	Seawater at High T,p	7 356	4 308	68
Wright et al. (2011)	Density Salinity	5 268	2 891	49
Marion et al. (2009)	$CaCO_3$ Solubility	5 169	3 170	36
Pawlowicz (2010)	Composition Variation	4 471	2 666	27
Feistel et al. (2010d)	SIA Library Equations	4 255	2 416	23
Wright et al. (2010)	SIA Library Routines	4 049	1 733	19
Feistel et al. (2008b)	Consistent New Potentials	3 585	1 527	27
Seitz et al. (2011)	Salinity Traceability	3 363	1 705	24
Feistel et al. (2010b)	Baltic Property Anomalies	3 183	1 500	12
Tailleux (2009)	Mixing Efficiency	2 752	1 303	11
Millero and Huang (2010)	Seawater at High T,S (corrig.)	2 189	909	1

864

865 **Table A2**: Metrics published by March 2024 of selected TEOS-10 related articles apart from *Ocean*
866 *Science.* "Ice Ih" is the ambient, hexagonal ice I phase of water.

Reference	Topic	Accessed	PDF Downloads	Cited
Wagner and Pruß (2002)	Water Helmholtz Function	7 516	7 516	3 457
Lemmon et al. (2000)	Dry Air Helmholtz Function	2 279	2 279	381
McDougall (2003)	Potential Enthalpy	1 970	1 367	50
Wagner et al. (2011)	Ice Melting/Sublimation	1 467	510	102
Seitz et al. (2010)	Salinity Determination	1 332		15
Feistel (2008b)	IAPWS-06 and IAPWS-08	1 279		4
Millero et al. (2008)	Seawater Composition	970		780
Feistel and Wagner (2006)	Ice Ih Gibbs Function	843	843	286
Feistel and Wagner (2005)	Ice Ih Gibbs Function	833		58
Graham and McDougall (2013)	Conservative Temperature	651	467	28

Feistel (2012)	New TEOS-10 Standard	436		27
Feistel (2008a)	Seawater Gibbs Function	134		133
Roquet et al. (2015)	TEOS-10 Polynomials	111		97
Feistel and Wagner (2007)	Ice Ih Sublimation >20 K	105		112
Feistel (2003)	Seawater Gibbs Function	100		105
McDougall et al. (2013)	Thermodynamics of Seawater	35		10
Feistel and Marion (2007)	Seawater Gibbs-Pitzer	25		32
Valladares et al. (2011)	Replacement of EOS-80	14+5		4+1

867

868 **Table A3**: IAPWS documents supporting TEOS-10, openly accessible at www.iapws.org. IAPWS
869 documents are independently and painstakingly verified before they may become adopted at an
870 annual meeting. No metrics available.

Document	Code	Topic	Meeting	Year
Release	R06-95	Water Helmholtz Function	Dresden	2016
Release	R10-06	Ice Ih Gibbs Function	Doorwerth	2009
Release	R13-08	Seawater Gibbs Function	Berlin	2008
Release	R14-08	Ice Melting/Sublimation	Pilsen	2011
Suppl. Release	SR1-86	Water Saturation Properties	St. Petersburg	1992
Suppl. Release	SR6-08	Liquid Water at 0.1 MPa	Pilsen	2011
Suppl. Release	SR7-09	Liquid Water Gibbs Function	Doorwerth	2009
Guideline	G05-01	Fundamental Constants	Virtual Online	2020
Guideline	G08-10	Humid Air Helmholtz Function	Niagara Falls	2010
Guideline	G09-12	Cold Water Vapour < 130 K	Boulder	2012
Guideline	G11-15	Fugacity Virial Equation	Stockholm	2015
Guideline	G12-15	Supercooled Water	Stockholm	2015
Advisory Note	AN4-09	IAPWS/CIPM Water Density	Doorwerth	2009
Advisory Note	AN5-13	Industrial Seawater	Dresden	2016
Advisory Note	AN6-16	IAPWS support for TEOS-10	Dresden	2016

871

872 **Table A4:** Numbers of unique internet downloads 2011-2023 of supporting material from the TEOS-
873 10 homepage at www.teos-10.org. "GSW" stands for the TEOS-10 Gibbs Seawater open source code
874 library. Data from Pawlowicz (2023)

Item	2011-13	2013-14	2014-15	2015-16	2016-17	2017-18	2018-19	2019-20	2020-21	2021-22	2022-23
TEOS-10 Manual	920	360	535	552	418	427	349	472	479	482	530
Getting Started	879	362	558	547	427	475	349	444	460	483	479
Lecture Slides	704	284	374	318	219	248	204	272	272	231	272
TEOS-10 Primer	584	197	289	297	222	217	187	253	260	226	268
GSW MATLAB	1920	1102	1485	1814	1235	1552	1233	1556	1504	1747	1897
GSW FORTRAN	366	222	171	162	127	116	82	98	83	92	87
GSW C	202	84	133	151	85	96	59	81	58	49	57
GSW PHP	-	55	61	43	29	60	28	52	22	22	21

SIA VB	72	100	46	45	45	48	43	47	47	38	30
SIA FORTRAN	59	118	58	44	36	42	37	42	31	33	31

875

876   **Table A5**: Selected additional TEOS-10 related readings, metrics by March 2024

Reference	Topic	Accessed	PDF Downloads	Cited
Turner et al. (2016)	Seawater Pitzer Model	13 780	1 175	21
Lovell-Smith et al. (2016)	Relative Humidity Challenges		6 502	27
Schmidt et al. (2018)	Density-Salinity Relation	9 421	5 481	28
Feistel et al. (2016a)	Challenges beyond TEOS-10		5 023	49
Dickson et al. (2016)	Seawater pH Challenges		2 818	43
Pawlowicz et al. (2016)	Seawater Salinity Challenges		2 738	40
Foken et al. (2021)	Atmospheric Measurements	5 709		2
Feistel (2018)	TEOS-10 Review	5 441	1 632	38
Feistel and Hellmuth (2023)	Dalton Equation	5 068		1
McDougall et al. (2021)	Ocean Heat Flux and Content	4 993	1 425	5
Hellmuth et al. (2020)	Ice-Crystal Nucleation	4 811		6
Uchida et al. (2019)	Optical Density Sensor	3 513		19
Hellmuth et al. (2021)	Mass Density of Humid Air	2 643		4
Feistel and Lovell-Smith (2017)	Relative Fugacity Part 1		1 335	18
Le Menn et al. (2018)	Seawater Salinity Measurands		1 136	13
Schmidt et al. (2016)	Seawater Density up to 1 ppm		950	21
Von Rohden et al (2016)	Baltic Sound Speed	2 122	784	1
Feistel et al. (2016b)	Uncertainty of Correlation Eqs.		662	14
Martins and Cross (2022)	TEOS-10 Excel Code	2 087	542	2
Hellmuth and Feistel (2020)	Low-Density Subcooled Water	1 827		1
McDougall et al. (2014)	Sea Ice Formation	1 124	771	16
Feistel and Hellmuth (2024a)	Evaporation Entropy	1 038		0
Harvey et al. (2023)	Water Properties	874	369	9
Uchida et al. (2020)	Seawater Intercomparison	707	764	6
Sharkawy et al. (2010)	Review of Seawater Correlations	701		946
Feistel (2018)	Relative Fugacity Part 2		267	3
Feistel et al. (2022)	Relative Fugacity Part 3		252	4
McDougall et al. (2023)	Seawater Potential of (S, CT, p)	629	122	1
Feistel et al. (2015)	Virial Fugacity Equation	581		17
Nayar et al. (2016)	Seawater Property Review	553		366
Marion et al. (2011)	Seawater pH	491		170
Roquet et al. (2015)	Seawater Density Polynomials	111		97
Pawlowicz and Feistel (2012)	TEOS-10 in Limnology			22
Kretzschmar et al. (2015)	Industrial Seawater Equation	104		0
Almeida et al. (2018)	TEOS-10 Atlantic Impact	53		5
Safarov et al. (2012)	High-Salinity Seawater	42		21
Woosley et al. (2014)	World Ocean Absolute Salinity	39		16
Safarov et al. (2013)	Brackish Seawater Properties	35		15
Ulfsbo et al. (2015)	Seawater Activity Coefficients	34		11
Feistel and Hagen (1998)	Sea Ice Gibbs Function	24		31
Feistel (2010)	Seawater Gibbs Function	23		24
Millero and Huang (2011)	Seawater Compressibility	19		19

Von Rohden et al. (2015)	Seawater Sound Speed 0.1 MPa			18
Budéus (2018)	TEOS-10 Density Bias ?	8		5
Lago et al. (2015)	Seawater Sound Speed < 70 MPa	8		4
Weinreben and Feistel (2019)	Anomalous Salinity Density	8		1
Waldmann et al. (2022)	Uncertainty of Ocean Variables	2		
Laliberte (2015)	TEOS-10 Python Code			

877

878 **Appendix B: Thermodynamic Potentials**

879 This Appendix provides a short introduction to thermodynamic potentials, supporting the equations
880 and topics discussed in this article. Alternative presentations from different perspectives are
881 available from numerous textbooks such as Guggenheim (1949), Margenau and Murphy (1964),
882 Landau and Lifschitz (1966) or Kittel (1969).

883 A key theoretical tool for the physical investigation of the globally warming climate and the related
884 energy balances is *thermodynamics*. It is known from experience that there exists a distinguished
885 state of various ambient substances that is known as a *thermodynamic equilibrium state*. If a sample
886 of matter is in this state, it may never spontaneously alter its measurable macroscopic properties
887 unless it becomes disturbed by external contact and exchange of energy or matter with its
888 surrounding. Typical properties which characterise a particular equilibrium state are the total mass of
889 a sample, m, its volume, V, its temperature, T, or its pressure, p. Of a given sample, different
890 equilibrium states may exist that differ in those quantities, but there exists a specific relation
891 between those variables, known as an *equation of state*, which is characteristic for the given
892 substance and remains universally valid at any of its possible equilibrium states. The most general
893 and comprehensive equation of state of a given substance is a *thermodynamic potential* of that
894 substance.

895 Thermodynamics is a mathematical theory for the construction and exploitation of equations of state
896 and of properties derived thereof for the prediction or verification of observations or experiments.
897 Depending on the properties of interest, equations of state may be formulated in various different
898 mathematical forms. It was discovered by J. Willard Gibbs (1873) that from a suitable thermodynamic
899 potential all thermodynamic properties of a given substance at any of its equilibrium states can be
900 derived by appropriate mathematical methods.

901 For theoretical reasons (namely, the statistical so-called *canonical ensemble*), a preferred
902 thermodynamic potential of a pure substance is its *Helmholtz Energy*, or *Free Energy*, $F(m, T, V)$,
903 expressed in terms of the sample's mass, m, its temperature und volume. For mixtures, the single
904 mass must be replaced by the set of partial masses of the species involved. Here, mass is used as a
905 measure for the amount of substance, rather than particle or mole numbers, for the practical reason
906 that in oceanography masses are easier measured than moles, and so TEOS-10 is following that
907 tradition and is a mass-based description. Classical empirical thermodynamics is independent of the
908 existence and properties of atoms or molecules which presently define the mole (BIPM 2019).

909 To the total energy E of the sample, the Helmholtz energy is related by the Helmholtz Differential
910 Equation,

911
$$E = F - T \left(\frac{\partial F}{\partial T} \right)_{m,V} \tag{B.1}$$

912 The potential function F is extensive, which means that for instance $F(2\,m, T, 2\,V) = 2\,F(m, T, V)$ is
913 valid for an equilibrium sample of twice the mass. It follows that the mass-specific Helmholtz
914 function, $F/m \equiv f(T, \rho)$, depends on two variables only, T and the mass density, $\rho \equiv m/V$, and is

915 mathematically simpler and more convenient than F, which may always be retrieved from a given f
916 by

917 $$F(m, T, V) = m \times f\left(T, \frac{m}{V}\right). \tag{B.2}$$

918 The quantitative description of a substance of interest in the form of a thermodynamic potential such
919 as $f(T, \rho)$ has axiomatic properties. The description is *complete*, i.e., all thermodynamic properties of
920 that substance are available, it is *consistent*, i.e., for any property one and only one result can be
921 derived, and it is *independent*, i.e., no part of this description may be omitted without loosing the
922 completeness. It is obvious that such axiomatic properties are very desirable for the description of
923 geophysical substances, however, such thermodynamic potentials are rarely found in the
924 corresponding literature. In particular in climate research which combines results and data from
925 different disciplines, such as meteorology and oceanography, from research carried out all over the
926 globe and over the years by subsequent generations of specialists, international binding standards
927 such as the International System of Units (SI) are required that ensure mutual consistency and
928 metrological comparability of any involved data produced from experiments, observations and
929 models.

930 Gibbs' (1873a) original potential function was (internal) energy, $e = E/m$. It is known that a sample's
931 energy can be increased by compression, $-p\mathrm{d}v$, where $v = 1/\rho$ is the specific volume, or by input of
932 heat, $T\mathrm{d}\eta$, where $\eta = N/m$ is the specific entropy. As an extensive quantity, entropy introduced by
933 Clausius (1865, 1976) is denoted here by N to avoid confusion with seawater salinity, *S*. Energy
934 conservation implies that

935 $$\mathrm{d}e = T\mathrm{d}\eta - p\mathrm{d}v. \tag{B.3}$$

936 Any such change between different equilibrium states of the same sample takes place along a
937 definite, substance-specific surface $e(\eta, v)$ so that $\mathrm{d}e$ in eq. (B.3) is mathematically an exact
938 differential and the partial derivatives of *e* possess the physical meanings that

939 $$T = \left(\frac{\partial e}{\partial \eta}\right)_v, \qquad -p = \left(\frac{\partial e}{\partial v}\right)_\eta. \tag{B.4}$$

940 Gibbs (1873b) also demonstrated that for several equilibrium samples in contact with one another, in
941 absence of gravity or accelerated motion, the samples are in mutual equilibrium only if they have
942 equal values of the coefficients T and p of eq. (2.3).

943 In the geophysical practice, the quantities η and v are difficult to measure, in contrast to, say, T or p.
944 Mathematically equivalent to $e(\eta, v)$, thermodynamic potentials in terms of the other three possible
945 pairs of independent variables are formally obtained from so-called Legendre transforms (Alberty
946 2001), namely the *Helmholtz function* $f(T, v) \equiv e - T\eta$ with the differential

947 $$\mathrm{d}f = -\eta\mathrm{d}T - p\mathrm{d}v, \tag{B.5}$$

948 the *Gibbs function* $g(T, p) \equiv f + pv = e - T\eta + pv$ with

949 $$\mathrm{d}g = -\eta\mathrm{d}T + v\mathrm{d}p, \tag{B.6}$$

950 and the specific *enthalpy* $h(\eta, p) \equiv g + T\eta = f + T\eta + pv = e + pv$ with

951 $$\mathrm{d}h = T\mathrm{d}\eta + v\mathrm{d}p. \tag{B.7}$$

952 Depending on the application purpose, each of these potential functions has certain advantages and
953 disadvantages, and having all of them optionally at hand in mutually consistent versions is most
954 useful.

955 Gibbs (1874-78) also considered a situation in which a given sample may exchange substance with its
956 surrounding. If the exchanged mass of substance i is $\mathrm{d}m_i$, the related change of the sample's
957 (extensive) energy E at constant entropy and volume is termed the *chemical potential* μ_i of that
958 substance,

959 $$\mathrm{d}E = T\mathrm{d}N - p\mathrm{d}V + \sum_i \mu_i\, \mathrm{d}m_i,$$ (B.8)

960 so that this exact differential implies that the chemical potential is obtained from

961 $$\mu_i \equiv \left(\frac{\partial E}{\partial m_i}\right)_{N,V,m_{j\neq i}} = \left(\frac{\partial F}{\partial m_i}\right)_{T,V,m_{j\neq i}} = \left(\frac{\partial G}{\partial m_i}\right)_{T,p,m_{j\neq i}} = \left(\frac{\partial H}{\partial m_i}\right)_{N,p,m_{j\neq i}}.$$ (B.9)

962 Equilibrium of a spatially extended substance, in absence of gravity or accelerated motion, requires
963 that in addition to T and p, also the chemical potential μ_i separately for each present substance
964 needs to possess the same value anywhere in the volume. "The potential for each component
965 substance must be constant throughout the whole mass" (Gibbs 1874-78: p. 119).

966 As intensive properties, the specific energies cannot depend on the total mass but only on the mass
967 fractions, $w_i \equiv m_i/m$. Because by definition $\sum w_i = 1$, only $(n-1)$ different fractions may be
968 independent variables describing the n components of a mixture. For example, one of the
969 components may be chosen as a master species, "0", such as a solvent, and the remaining ones, $i =$
970 $1, \dots, n-1$, may denote the solutes.

971 In terms of T and p, chemical potentials are computed from the Gibbs function, g, through the Gibbs
972 energy, G, of eq. (B.9). Because the Gibbs function depends only on the independent intensive
973 variables, $g(w_i, T, p)$, the solutes' chemical potentials, $i > 0$, are

974 $$\mu_i = \left(\frac{\partial G}{\partial m_i}\right)_{T,p,m_{j\neq i}} = \left(\frac{\partial (m\,g)}{\partial m_i}\right)_{T,p,m_{j\neq i}} = g + \left(\frac{\partial g}{\partial w_i}\right)_{T,p,w_{j\neq i}} - \sum_{j=1}^{n-1} w_j \left(\frac{\partial g}{\partial w_j}\right)_{T,p,w_{k\neq j}}$$ (B.10)

975 Similarly, the solvent's chemical potential is

976 $$\mu_0 = \left(\frac{\partial G}{\partial m_0}\right)_{T,p,m_{j>0}} = \left(\frac{\partial (m\,g)}{\partial m_0}\right)_{T,p,m_{j>0}} = g - \sum_{j=1}^{n-1} w_j \left(\frac{\partial g}{\partial w_j}\right)_{T,p,w_{j>0}}.$$ (B.11)

977 Therefore, the *relative chemical potentials* of the solutes are simply the partial derivatives,

978 $$\mu_i - \mu_0 = \left(\frac{\partial g}{\partial w_i}\right)_{T,p,w_{j\neq i}}.$$ (B.12)

979 For mixtures, $n > 1$, the differential (B.6) of the Gibbs function takes the more general form

980 $$\mathrm{d}g = -\eta \mathrm{d}T + v\mathrm{d}p + \sum_{i=1}^{n-1} (\mu_i - \mu_0)\mathrm{d}w_i.$$ (B.13)

981 It follows straightforwardly from (B.10), (B.11) that the sum,

982 $$\sum_{i=0}^{n-1} \mu_i\, m_i = m\, g = G,$$ (B.14)

983 equals the Gibbs energy itself (Gibbs 1874-78: eq. (96) therein, Guggenheim 1949, Landau and
984 Lifschitz 1966, Kittel 1969). In particular, if $n = 1$, the Gibbs function g of a pure substance
985 represents its chemical potential,

986 $$g = \mu.$$ (B.15)

987 Where two phases of a pure substance are in contact at mutual equilibrium, such as saturated water
988 vapour at the liquid water surface, the mathematically distinct Gibbs functions of those phases take
989 equal values. This indispensable condition for mutual consistency between the thermodynamic

potentials of TEOS-10 is rigorously obeyed by virtue of appropriate reference-state conditions (Feistel et al. 2008b).

Competing interests. The author has declared that he has no competing interests.

Acknowledgements. The author is grateful to Karen Heywood for her kind invitation to write this Ocean Science Jubilee article. This paper contributes to the tasks of the Joint SCOR/IAPWS/IAPSO Committee on the Properties of Seawater (JCS).

References

Abraham, J.P., Baringer, M., Bindoff, N.L., Boyer, S.T., Cheng, L.J., Church, J.A., Conroy, J.L., Domingues, C.M., Fasullo, J.T., Gilson, J., Goni, G., Good, S.A., Gorman, J.M., Gouretski, V., Ishii, M., Johnson, G.C., Kizu, S., Lyman, J.M., Macdonald, A.M., Minkowycz, W.J., Moffitt, S.E., Palmer, M.D., Piola, A.R., Reseghetti, F., Schuckmann, K., Trenberth, K.E., Velicogna, I., and Willis, J.K.: A Review of Global Ocean Temperature Observations: Implications for Ocean Heat Content Estimates and Climate Change, Reviews of Geophysics 51, 450-483, https://doi.org/10.1002/rog.20022, 2013.

Alberty, R.A.: Use of Legendre transforms in chemical thermodynamics, Pure Appl. Chem. 73, 1349–1380, https://doi.org/10.1351/pac200173081349, 2001.

Albrecht, F.: Untersuchungen über den Wärmehaushalt der Erdoberfläche in verschiedenen Klimagebieten, Reichsamt für Wetterdienst, Wissenschaftliche Abhandlungen Bd. VIII, Nr. 2, Springer, Berlin, Heidelberg, https://doi.org/10.1007/978-3-662-42530-5, 1940.

Allen, J. and Ward, K.: Cloudy Earth. NASA Earth Observatory image using data provided by the MODIS Atmosphere Science Team, NASA Goddard Space Flight Center, https://earthobservatory.nasa.gov/images/85843/cloudy-earth, 2015.

Almeida, L., Lima de Azevedo, J.L., Kerr, R., Araujo, M., and Mata, M.M.: Impact of the new equation of state of seawater (TEOS-10) on the estimates of water mass mixture and meridional transport in the Atlantic Ocean, Progress in Oceanography 162, 13-24, https://doi.org/10.1016/j.pocean.2018.02.008, 2018.

Azorin-Molina, C., Dunn, R.J.H., Ricciardulli, L., Mears, C.A., Nicolas, J.P., McVicar, T.R., Zeng, Z., and Bosilovich, M.G.: Land and Ocean Surface Winds, in: Blunden, J., Boyer, T., Bartow-Gillies, E. (eds.): State of the Climate in 2022, Bull. Amer. Meteor. Soc. 104, S72–S74, https://doi.org/10.1175/BAMS-D-23-0090.1, 2023.

Baumgartner, A. and Reichel, E.: The World Water Balance, R. Oldenbourg Verlag, München, Germany, 1975.

BIPM: The International System of Units (SI), Bureau International des Poids et Mesures, Sèvres, https://www.bipm.org/en/publications/si-brochure , 2019.

Budéus, G. Th.: Potential bias in TEOS10 density of sea water samples, Deep-Sea Res. Pt. I, 134, 41–47, https://doi.org/10.1016/j.dsr.2018.02.005, 2018.

Budyko, M.I.: Evolyutsiya Biosfery, Gidrometeoizdat, Leningrad, 1984.

Carlon, H.R.: Infrared emission by fine water aerosols and fogs, Appl. Opt. 9, 2000-2006, https://doi.org/10.1364/AO.9.002000, 1970.

1030 Carlon, H.R.: Aerosol spectrometry in the infrared, Appl. Opt. 19, 2210-2218,
1031 https://doi.org/10.1364/AO.19.002210, 1980.

1032 Cheng, L., Abraham, J., Trenberth, K.E., Boyer, T., Mann, M.E., Zhu, J., Wang, F., Yu, F., Locarnini, R.,
1033 Fasullo, J., Zheng, F., Li, Y., Zhang, B., Wan, L., Chen, X., Wang, D., Feng, L., Song, X., Liu, Y.,
1034 Reseghetti, F., Simoncelli, S., Gouretski, V., Chen, G., Mishonov, A., Reagan, J., Von Schuckmann, K.,
1035 Pan, Y., Tan, Z., Zhu, Y., Wei, W., Li, G., Ren, Q., Cao, L., and Lu, Y.: New record ocean temperatures
1036 and related climate indicators in 2023, Advances in Atmospheric Sciences,
1037 https://doi.org/10.1007/s00376-024-3378-5, 2024.

1038 Clausius, R.: Ueber verschiedene für die Anwendung bequeme Formen der Hauptgleichungen der
1039 mechanischen Wärmetheorie, Annalen der Physik 201, 353–400,
1040 https://doi.org/10.1002/andp.18652010702, 1865.

1041 Clausius, R.: Die Mechanische Wärmetheorie, Friedrich Vieweg, Braunschweig, 1876.

1042 Dai, A.: Recent Climatology, Variability, and Trends in Global Surface Humidity, J. Clim. 19, 3589–
1043 3606, https://doi.org/10.1175/JCLI3816.1, 2006.

1044 Debski, K.: Continental Hydrology, Volume 2: Physics of Water, Atmospheric Precipitation, and
1045 Evaporation, Scientific Publications Foreign Cooperation Center of the Central Institute, Warsaw,
1046 1966.

1047 Dickson, A.G., Camões, M.F., Spitzer, P., Fisicaro, P., Stoica, D., Pawlowicz, R., and Feistel, R.:
1048 Metrological challenges for measurements of key climatological observables, Part 3: Seawater pH,
1049 Metrologia 53, R26–R39, https://doi.org/10.1088/0026-1394/53/1/R26 , 2016.

1050 Eastman, R., Warren, S.G., and Hahn, C.J.: Variations in Cloud Cover and Cloud Types over the Ocean
1051 from Surface Observations, 1954–2008, J. Climate 24, 5914-5934,
1052 https://doi.org/10.1175/2011JCLI3972.1, 2011.

1053 Ebeling, W. and Feistel, R.: Physik der Selbstorganisation und Evolution. Akademie-Verlag, Berlin,
1054 1982.

1055 Emden, R.: Über Strahlungsgleichgewicht und atmosphärische Strahlung, Sitzungsber. Akad. Wiss.
1056 München 1, 55-142, https://www.zobodat.at/pdf/Sitz-Ber-Akad-Muenchen-math-Kl_1913_0001.pdf ,
1057 1913.

1058 Falkenhagen, H., Ebeling, W., and Hertz, H.G.: Theorie der Elektrolyte, S. Hirzel Verlag, Leipzig, 1971.

1059 Fasullo, J.T. and Trenberth, K.E.: A Less Cloudy Future: The Role of Subtropical Subsidence in Climate
1060 Sensitivity, Science 338, 792-794, https://doi.org/10.1126/science.1227465, 2012.

1061 Feistel, R.: Thermodynamics of Seawater, in: Striggow, K. Schröder, A. (eds.): German Democratic
1062 Republic National Report for the period 1.1.1987–2.10.1990 (Final Report) IAPSO, presented at the
1063 XX. General Assembly of the IUGG, Wien 1991, Institut für Meereskunde, Warnemünde,
1064 https://doi.org/10.13140/RG.2.1.3973.3282, 1991.

1065 Feistel, R.: Equilibrium thermodynamics of seawater revisited, Prog. Oceanogr. 31, 101–179,
1066 https://doi.org/10.1016/0079-6611(93)90024-8, 1993.

1067 Feistel, R.: A new extended Gibbs thermodynamic potential of seawater, Progress in Oceanography
1068 58, 43-114, https://doi.org/10.1016/S0079-6611(03)00088-0, 2003.

1069 Feistel, R.: A Gibbs function for seawater thermodynamics for −6 to 80°C and salinity up to 120 g kg^{-1},
1070 Deep Sea Research Part I 55, 1639-1671, https://doi.org/10.1016/j.dsr.2008.07.004, 2008a.

Feistel, R.: Thermodynamics of water, vapor, ice, and seawater, Accred. Qual. Assur. 13, 593–599, https://doi.org/10.1007/s00769-008-0443-1, 2008b.

Feistel, R.: Extended equation of state for seawater at elevated temperature and salinity, Desalination 250, 14–18, https://doi.org/10.1016/j.desal.2009.03.020, 2010.

Feistel, R.: Radiative entropy balance and vertical stability of a gray atmosphere, Eur. Phys. J. B 82, 197–206, https://doi.org/10.1140/epjb/e2011-20328-2, 2011.

Feistel, R.: TEOS-10: A New International Oceanographic Standard for Seawater, Ice, Fluid Water, and Humid Air, Int. J. Thermophys. 33, 1335–1351, https://doi.org/10.1007/s10765-010-0901-y, 2012.

Feistel, R.: Salinity and relative humidity: Climatological relevance and metrological needs, Acta Imeko 4, 57–61, http://dx.doi.org/10.21014/acta_imeko.v4i4.216, 2015.

Feistel, R.: Thermodynamic properties of seawater, ice and humid air: TEOS-10, before and beyond, Ocean Sci. 14, 471–502, https://doi.org/10.5194/os-14-471-2018, 2018.

Feistel, R.: Distinguishing between Clausius, Boltzmann and Pauling Entropies of Frozen Non-Equilibrium States, Entropy 21, 799, https://doi.org/10.3390/e21080799, 2019.

Feistel, R.: On the Evolution of Symbols and Prediction Models, Biosemiotics 16, 311–371, https://doi.org/10.1007/s12304-023-09528-9, 2023.

Feistel, R. and Ebeling, W.: Physics of Self-Organization and Evolution, Wiley-VCH, Weinheim, 2011.

Feistel, R. and Hagen, E.: On the GIBBS thermodynamic potential of seawater, Prog. Oceanogr. 36, 249–327, https://doi.org/10.1016/S0165-232X(98)00014-7, 1995.

Feistel, R. and Hagen, E.: A Gibbs thermodynamic potential of sea ice, Cold Regions Science and Technology 28, 83–142, https://doi.org/10.1016/S0165-232X(98)00014-7, 1998.

Feistel, R. and Hellmuth, O.: Relative Humidity: A Control Valve of the Steam Engine Climate, J. Hum. Earth Future 2, 140–182, https://doi.org/10. 28991/HEF-2021-02-02-06, 2021.

Feistel, R. and Hellmuth, O.: Thermodynamics of Evaporation from the Ocean Surface, Atmosphere 14, 560, https://doi.org/10.3390/atmos14030560, 2023.

Feistel, R. and Hellmuth, O.: Irreversible Thermodynamics of Seawater Evaporation, J. Mar. Sci. Eng. 12, 166, https://doi.org/10.3390/jmse12010166, 2024a.

Feistel, R. and Hellmuth, O.: TEOS-10 Equations for the Lifted Condensation Level (LCL) and Climatic Feedback of Marine Clouds, Preprints 2024031171, https://doi.org/10.20944/preprints202403.1171.v1, 2024b.

Feistel, R., Hellmuth, O. and Lovell-Smith, J.: Defining relative humidity in terms of water activity. III: Relations to dew-point and frost-point temperatures, Metrologia 59, 045013, https://doi.org/10.1088/1681-7575/ac7185, 2022.

Feistel, R. and Lovell-Smith, J.W.: Defining relative humidity in terms of water activity. Part 1: definition, Metrologia 54, 566–576, https://doi.org/10.1088/1681-7575/aa7083, 2017.

Feistel, R., Lovell-Smith, J.W., and Hellmuth, O.: Virial Approximation of the TEOS-10 Equation for the Fugacity of Water in Humid Air, Int. J. Thermophys. 36, 44–68, https://doi.org/10.1007/s10765-014-1784-0, 2015.

1109 Feistel, R., Lovell-Smith, J.W., Saunders, P., and Seitz, S.: Uncertainty of empirical correlation
1110 equations, Metrologia 53, 1079, https://doi.org/10.1088/0026-1394/53/4/1079, 2016.

1111 Feistel, R. and Marion, G.M.: A Gibbs–Pitzer function for high-salinity seawater thermodynamics,
1112 Prog. Oceanogr. 74, 515–539, https://doi.org/10.1016/j.pocean.2007.04.020, 2007.

1113 Feistel, R., Marion, G.M., Pawlowicz, R., and Wright, D.G.: Thermophysical property anomalies of
1114 Baltic seawater, Ocean Sci. 6, 949–981, https://doi.org/10.5194/os-6-949-2010, 2010b.

1115 Feistel, R., Tailleux, R., and McDougall, T. (eds.): Thermophysical Properties of Seawater, Copernicus,
1116 Göttingen, Germany, https://os.copernicus.org/articles/special_issue14.html, 2008a.

1117 Feistel, R. and Wagner, W.: High-pressure thermodynamic Gibbs functions of ice and sea ice, J. Mar.
1118 Res. 63, 95–139, https://elischolar.library.yale.edu/journal_of_marine_research/73 , 2005. [former
1119 DOI: 10.1357/0022240053693789 is invalid now]

1120 Feistel, R. and Wagner, W.: A new equation of state for H2O ice Ih, J. Phys. Chem. Ref. Data 35, 1021–
1121 1047, https://doi.org/10.1063/1.2183324, 2006.

1122 Feistel, R. and Wagner, W.: Sublimation pressure and sublimation enthalpy of H_2O ice Ih between 0
1123 and 273.16 K, Geochim. Cosmochim. Acta 71, 36–45, https://doi.org/10.1016/j.gca.2006.08.034,
1124 2007.

1125 Feistel, R., Weinreben, S., Wolf, H., Seitz, S., Spitzer, P., Adel, B., Nausch, G., Schneider, B., and
1126 Wright, D.G.: Density and Absolute Salinity of the Baltic Sea 2006–2009, Ocean Sci. 6, 3–24,
1127 https://doi.org/10.5194/os-6-3-2010, 2010c.

1128 Feistel, R., Wielgosz, R., Bell, S.A., Camões, M.F., Cooper, J.R., Dexter, P., Dickson, A.G., Fisicaro, P.,
1129 Harvey, A.H., Heinonen, M., Hellmuth, O., Kretzschmar, H.-J., Lovell-Smith, J.W., McDougall, T.J.,
1130 Pawlowicz, R., Ridout, R., Seitz, S., Spitzer, P., Stoica, D., and Wolf, H.: Metrological challenges for
1131 measurements of key climatological observables: Oceanic salinity and pH, and atmospheric humidity.
1132 Part 1: overview, Metrologia 53, R1–R11, https://doi.org/10.1088/0026-1394/53/1/R1, 2016a.

1133 Feistel, R., Wright, D.G., Jackett, D.R., Miyagawa, K., Reissmann, J.H., Wagner, W., Overhoff, U.,
1134 Guder, C., Feistel, A., and Marion, G.M.: Numerical implementation and oceanographic application of
1135 the thermodynamic potentials of liquid water, water vapour, ice, seawater and humid air – Part 1:
1136 Background and equations, Ocean Sci. 6, 633–677, https://doi.org/10.5194/os-6-633-2010, 2010d.

1137 Feistel, R., Wright, D.G., Kretzschmar, H.-J., Hagen, E., Herrmann, S., and Span, R.: Thermodynamic
1138 properties of sea air, Ocean Sci. 6, 91–141, https://doi.org/10.5194/os-6-91-2010, 2010a.

1139 Feistel, R., Wright, D.G., Miyagawa, K., Harvey, A.H., Hruby, J., Jackett, D.R., McDougall, T.J., and
1140 Wagner, W.: Mutually consistent thermodynamic potentials for fluid water, ice and seawater: a new
1141 standard for oceanography, Ocean Sci. 4, 275–291, https://doi.org/10.5194/os-4-275-2008, 2008b.

1142 Flohn, H., Kapala, A., Knoche, H.R., and Mächel, H.: Water vapour as an amplifier of the greenhouse
1143 effect: new aspects, Meteorol. Zeitschrift, N.F. 1, 120-138,
1144 https://doi.org/10.1127/metz/1/1992/122, 1992.

1145 Fofonoff, N.P. and Millard Jr., R.C.: Algorithms for computation of fundamental properties of
1146 seawater, Unesco technical papers in marine science 44, Unesco, Paris,
1147 https://darchive.mblwhoilibrary.org/server/api/core/bitstreams/f77d18e9-e756-58eb-b042-
1148 a8870de55e3b/content, 1983.

1149   Foken, T., Hellmuth, O., Huwe, B., and Sonntag, D.: Physical Quantities, in: Foken, T. (ed.): Springer
1150   Handbook of Atmospheric Measurements, Springer Handbooks, Springer, Cham, pp. 107–151,
1151   https://doi.org/10.1007/978-3-030-52171-4_5, 2021.

1152   Foster, M.J., Phillips, C., Heidinger, A.K., Borbas, E.E., Li, Y., Menzel, P., Walther, A., and Weisz, E.:
1153   PATMOS-x Version 6.0: 40 Years of Merged AVHRR and HIRS Global Cloud Data, J. Climate 36, 1143-
1154   1160, https://doi.org/10.1175/JCLI-D-22-0147.1, 2023.

1155   Gibbs, J.W.: Graphical methods in the thermodynamics of fluids, Transactions of the Connecticut
1156   Academy of Arts and Science 2, 309–342,
1157   https://www3.nd.edu/~powers/ame.20231/gibbs1873a.pdf, 1873a.

1158   Gibbs, J.W.: A Method of Graphical Representation of the Thermodynamic Properties of Substances
1159   by Means of Surfaces, Trans. Conn. Acad. Arts Sci. 2, 382–404,
1160   https://www3.nd.edu/~powers/ame.20231/gibbs1873b.pdf, 1873b.

1161   Gibbs, J.W.: On the equilibrium of heterogeneous substances, The Transactions of the Connecticut
1162   Academy of Arts and Science 3, 108–248, https://www.biodiversitylibrary.org/page/27725812, 1874-
1163   78.

1164   Gill, A.E.: Atmosphere-Ocean Dynamics, Academic Press, San Diego, 1982.

1165   Gimeno, L., Nieto, R., Drumond, A., and Durán-Quesada, A.M.: Ocean Evaporation and Precipitation,
1166   in: Orcutt, J. (ed.): Earth System Monitoring: Selected Entries from the Encyclopedia of Sustainability
1167   Science and Technology, Springer, New York, NY, USA, https://doi.org/10.1007/978-1-4614-5684-
1168   1_13, 2013.

1169   Glansdorff, P. and Prigogine, I.: Thermodynamic Theory of Structure, Stability and Fluctuations,
1170   Wiley-Interscience, London, 1971.

1171   Graham, F.S., and McDougall, T.J.: Quantifying the Nonconservative Production of Conservative
1172   Temperature, Potential Temperature, and Entropy, J. Phys. Oceanogr. 43, 838–862,
1173   https://doi.org/10.1175/JPO-D-11-0188.1, 2013.

1174   Guggenheim, E.A.: Thermodynamics, North-Holland, Amsterdam, 1949.

1175   Harvey, A.: Thermodynamic Properties of Water: Tabulation From the IAPWS Formulation 1995 for
1176   the Thermodynamic Properties of Ordinary Water Substance for General and Scientific Use, NIST
1177   Interagency/Internal Report (NISTIR), National Institute of Standards and Technology, Gaithersburg,
1178   MD, https://doi.org/10.6028/NIST.IR.5078, 1998.

1179   Harvey, A.H., Hrubý, J., and Meier, K.: Improved and Always Improving: Reference Formulations for
1180   Thermophysical Properties of Water, J. Phys. Chem. Ref. Data 52, 011501,
1181   https://doi.org/10.1063/5.0125524, 2023.

1182   Held, I.M. and Soden, B.J.: Robust Responses of the Hydrological Cycle to Global Warming, J. Climate
1183   19, 5686-5699, https://doi.org/10.1175/JCLI3990.1, 2006.

1184   Hellmuth, O. and Feistel, R.: Analytical Determination of the Nucleation-Prone, Low-Density Fraction
1185   of Subcooled Water, Entropy 22, 933, https://doi.org/10.3390/e22090933, 2020.

1186   Hellmuth, O., Feistel, R., and Foken, T.: Intercomparison of different state-of-the-art formulations of
1187   the mass density of humid air, Bull. Atmos. Sci. & Technol. 2, 13, https://doi.org/10.1007/s42865-
1188   021-00036-7, 2021.

1189   Hellmuth, O., Schmelzer, J.W.P., and Feistel, R.: Ice-Crystal Nucleation in Water: Thermodynamic
1190   Driving Force and Surface Tension. Part I: Theoretical Foundation, Entropy 22, 50,
1191   https://doi.org/10.3390/e22010050 , 2020.

1192   Hirota, N., Ogura, T., Shiogama, H., Caldwell, P., Watanabe, M., Kamae, Y., and Suzuki, K.:
1193   Underestimated marine stratocumulus cloud feedback associated with overly active deep convection
1194   in models, Environ. Res. Lett. 16, 074015, https://doi.org/10.1088/1748-9326/abfb9e, 2021.

1195   IAPWS AN6-16: Advisory Note No. 6: Relationship between Various IAPWS Documents and the
1196   International Thermodynamic Equation of Seawater—2010 (TEOS-10), The International Association
1197   for the Properties of Water and Steam, Dresden, Germany, http://www.iapws.org, 2016.

1198   IAPWS SR1-86: Revised Supplementary Release on Saturation Properties of Ordinary Water
1199   Substance, The International Association for the Properties of Water and Steam, St. Petersburg,
1200   Russia, http://www.iapws.org, 1992.

1201   IOC, SCOR, and IAPSO: The international thermodynamic equation of seawater – 2010: Calculation
1202   and use of thermodynamic properties, Intergovernmental Oceanographic Commission, Manuals and
1203   Guides No. 56, UNESCO (English), 196 pp., Paris,
1204   https://unesdoc.unesco.org/ark:/48223/pf0000188170, 2010.

1205   IOC-UNESCO: Resolution XXV-7 International Thermodynamic Equation of Seawater (TEOS-10), in:
1206   Proceedings of the Intergovernmental Oceanographic Commission, Twenty-Fifth Session of the
1207   Assembly, Paris, France, 16–25 June 2009,
1208   http://unesdoc.unesco.org/images/0018/001878/187890e.pdf, 2009.

1209   IUGG: Resolution 4: Adoption of the International Thermodynamic Equation of Seawater–2010
1210   (TEOS-10), In Proceedings of the International Union of Geodesy and Geophysics, XXV General
1211   Assembly, Melbourne, Australia, 27 June–7 July 2011, https://iugg.org/wp-
1212   content/uploads/2022/03/IUGG-Resolutions-XXV-GA-Melbourne-English.pdf, 2011.

1213   Josey, S.A., Gulev, S., and Yu, L.: Exchanges through the ocean surface, in: Siedler, G., Griffies, S.M.,
1214   Gould, J., and Church, J.A. (eds.): Ocean Circulation and Climate. A 21st Century Perspective,
1215   Elsevier, Amsterdam, The Netherlands, pp. 115–140, https://doi.org/10.1016/B978-0-12-391851-
1216   2.00005-2, 2013.

1217   Josey, S.A., Kent, E.C., and Taylor, P.K.: New Insights into the Ocean Heat Budget Closure Problem
1218   from Analysis of the SOC Air–Sea Flux Climatology, J. Climate 12, 2856-2880,
1219   https://doi.org/10.1175/1520-0442(1999)012<2856:NIITOH>2.0.CO;2, 1999.

1220   Kittel, C.: Thermal Physics, Wiley, New York, 1969.

1221   Köhler, H.: The nucleus in and the growth of hygroscopic droplets, Trans. Faraday Soc. 32, 1152–
1222   1161, https://doi.org/10.1039/tf9363201152, 1936.

1223   Kraus, E.B. and Businger, J.A.: Atmosphere–Ocean Interaction, Oxford University Press/Clarendon,
1224   New York, Oxford, 1994.

1225   Kretzschmar, H. J., Feistel, R., Wagner, W., Miyagawa, K., Harvey, A. H., Cooper, J. R., Hiegemann, M.,
1226   Blangettit, F.L., Orlov, K.A., Weber, I., Singh, A., and Herrmann, S.: The IAPWS industrial formulation
1227   for the thermodynamic properties of seawater, Desalination and Water Treatment 55, 1177–1199,
1228   https://doi.org/10.1080/19443994.2014.925838, 2015.

Lago, S., Giuliano Albo, P.A., von Rohden, C., and Rudtsch, S.: Speed of sound measurements in North Atlantic Seawater and IAPSO Standard Seawater up to 70 MPa, Marine Chemistry 177, 662-667, https://doi.org/10.1016/j.marchem.2015.10.007, 2015.

Laliberte, F.: Python bindings for TEOS-10, https://github.com/laliberte/pyteos_air, 2015.

Landau, L.D. and Lifschitz, E.M.: Statistische Physik, Akademie-Verlag, Berlin, 1966.

Landau, L.D. and Lifschitz, E.M.: Hydrodynamik, Akademie-Verlag, Berlin, 1974.

Le Menn, M., Giuliano Albo, P.A., Lago, S., Romeo, R., and Sparasci, F.: The absolute salinity of seawater and its measurands, Metrologia 56, 015005, https://doi.org/10.1088/1681-7575/aaea92 , 2018.

Lemmon, E.W., Jacobsen, R.T, Penoncello, S.G., and Friend, D.G.: Thermodynamic Properties of Air and Mixtures of Nitrogen, Argon, and Oxygen From 60 to 2000 K at Pressures to 2000 MPa, J. Phys. Chem. Ref. Data 29, 331, https://doi.org/10.1063/1.1285884, 2000.

Linke, F. and Baur, F.: Meteorologisches Taschenbuch, Geest & Portig, Leipzig, 1972.

Lovell-Smith, J.W., Feistel, R., Harvey, A.H., Hellmuth, O., Bell, S.A., Heinonen, M., and Cooper, J.R.: Metrological challenges for measurements of key climatological observables. Part 4: Atmospheric relative humidity, Metrologia 53, R39–R59, https://doi.org/10.1088/0026-1394/53/1/R40, 2016.

Margenau, H. and Murphy, G.M.: Die Mathematik für Physik und Chemie, B.G. Teubner, Leipzig, 1964.

Marion, G.M., Millero, F.J., and Feistel, R.: Precipitation of solid phase calcium carbonates and their effect on application of seawater S_A–T–P models, Ocean Sci. 5, 285–291, https://doi.org/10.5194/os-5-285-2009, 2009.

Marion, G.M., Millero, F.J., Camões, F., Spitzer, P., Feistel, R., and Chen, C.-T.A.: pH of Seawater, Mar. Chem., 126, 89–96, https://doi.org/10.1016/j.marchem.2011.04.002, 2011.

Martins, C.G. and Cross, J.: Technical note: TEOS-10 Excel – implementation of the Thermodynamic Equation Of Seawater – 2010 in Excel, Ocean Sci. 18, 627–638, https://doi.org/10.5194/os-18-627-2022, 2022.

McDougall, T.J.: Potential enthalpy: A conservative oceanic variable for evaluating heat content and heat fluxes, J. Phys. Oceanogr. 33, 945–963, https://doi.org/10.1175/1520-0485(2003)033<0945:PEACOV>2.0.CO;2, 2003.

McDougall, T.J., Feistel, R., and Pawlowicz, R.: Chapter 6 - Thermodynamics of Seawater, in: Siedler, G., Griffies, S.M., Gould, J., and Church, J.A. (eds.): Ocean Circulation and Climate - A 21st Century Perspective, Academic Press, Oxford, pp. 141-158, https://doi.org/10.1016/B978-0-12-391851-2.00006-4, 2013.

McDougall, T.J., Jackett, D.R., Millero, F.J., Pawlowicz, R., and Barker, P.M.: A global algorithm for estimating Absolute Salinity, Ocean Sci. 8, 1123–1134, https://doi.org/10.5194/os-8-1123-2012, 2012.

McDougall, T.J., Barker, P.M., Holmes, R.M., Pawlowicz, R., Griffies, S.M., and Durack, P.J.: The interpretation of temperature and salinity variables in numerical ocean model output and the calculation of heat fluxes and heat content, Geoscientific Model Development 14, 6445–6466, https://doi.org/10.5194/gmd-14-6445-2021, 2021.

McDougall, T.J., Barker, P.M., Feistel, R., and Galton-Fenzi, B.K.: Melting of Ice and Sea Ice into Seawater and Frazil Ice Formation, Journal of Physical Oceanography 44, 1751–1775, https://doi.org/10.1175/JPO-D-13-0253.1, 2014.

McDougall, T.J., Barker, P.M., Feistel, R., and Roquet, F.: A thermodynamic potential of seawater in terms of Absolute Salinity, Conservative Temperature, and in situ pressure, Ocean Sci. 19, 1719–1741, https://doi.org/10.5194/os-19-1719-2023 , 2023.

MetOffice: New marine surface humidity climate monitoring product, https://www.metoffice.gov.uk/research/news/2020/new-marine-surface-humidity-climate-monitoring-product, 2020.

Millero, F.J.: The thermodynamics of seawater. Part I. The PVT properties, Ocean Phys. Eng. 7, 403–460, https://www.researchgate.net/publication/289966693_THERMODYNAMICS_OF_SEAWATER_-_1_THE_PVT_PROPERTIES, 1982.

Millero, F.J.: The Thermodynamics of Seawater. Part II. Thermochemical Properties, Ocean Phys. Eng. 8, 1–40, https://www.researchgate.net/publication/289966823_THERMODYNAMICS_OF_SEAWATER_PART_II_THERMOCHEMICAL_PROPERTIES, 1983.

Millero, F.J.: History of the Equation of State of Seawater, Oceanography 23, 18-33, https://doi.org/10.5670/oceanog.2010.21, 2010.

Millero, F.J., Feistel, R., Wright, D.G., and McDougall, T.J.: The composition of Standard Seawater and the definition of the Reference-Composition Salinity Scale, Deep Sea Research Part I 55, 50-72, https://doi.org/10.1016/j.dsr.2007.10.001, 2008.

Millero, F.J. and Huang, F.: The density of seawater as a function of salinity (5 to 70 g kg^{-1}) and temperature (273.15 to 363.15 K), Ocean Sci. 5, 91–100, https://doi.org/10.5194/os-5-91-2009, 2009.

Millero, F. J. and Huang, F.: Corrigendum to "The density of seawater as a function of salinity (5 to 70 g kg^{-1}) and temperature (273.15 to 363.15 K)" published in Ocean Sci., 5, 91–100, 2009, Ocean Sci. 6, 379–379, https://doi.org/10.5194/os-6-379-2010, 2010.

Millero, F.J. and Leung, W.H.: The thermodynamics of seawater at one atmosphere, Am. J. Sci. 276, 1035–1077, https://doi.org/10.2475/ajs.276.9.1035, 1976.

Montgomery, R.B.: Observations of vertical humidity distribution above the ocean surface and their relation to evaporation, Pap. Phys. Oceanogr. Meteorol. 7, 2–30, https://doi.org/10.1575/1912/1099, 1940.

Morice, C.P., Kennedy, J.J., Rayner, N.A., and Jones, P.D.: Quantifying uncertainties in global and regional temperature change using an ensemble of observational estimates: The HadCRUT4 data set, J. Geophys. Res. 117, D08101, https://doi.org/10.1029/2011JD017187, 2012.

Muhlbauer, A., McCoy, I.L., and Wood, R.: Climatology of stratocumulus cloud morphologies: microphysical properties and radiative effects, Atmos. Chem. Phys. 14, 6695–6716, https://doi.org/10.5194/acp-14-6695-2014, 2014.

Mulligan, J.F. and Hertz, G.G.: An unpublished lecture by Heinrich Hertz: "On the energy balance of the Earth", American Journal of Physics 65, 36-45, https://doi.org/10.1119/1.18565, 1997.

Nayar, K.G., Sharqawy, M.H., Banchik, L.D., and Lienhard V, J.H.: Thermophysical properties of seawater: A review and new correlations that include pressure dependence, Desalination 390, 1-24, https://doi.org/10.1016/j.desal.2016.02.024, 2016.

Pawlowicz, R.: A model for predicting changes in the electrical conductivity, practical salinity, and absolute salinity of seawater due to variations in relative chemical composition, Ocean Sci. 6, 361–378, https://doi.org/10.5194/os-6-361-2010, 2010.

Pawlowicz, R.: Report to SCOR on JCS Activities Jun 2022 - Jun 2023, Joint SCOR/IAPWS/IAPSO Committee on the Properties of Seawater (JCS), https://scor-int.org/wp-content/uploads/2023/07/JCS-2023.pdf, 2023.

Pawlowicz, R. and Feistel, R.: Limnological applications of the Thermodynamic Equation of Seawater 2010 (TEOS-10), Limnology and Oceanography Methods 10, 853-867, https://doi.org/10.4319/lom.2012.10.853, 2012.

Pawlowicz, R., Feistel, R., McDougall, T.J., Ridout, P., Seitz, S., and Wolf, H.: Metrological challenges for measurements of key climatological observables. Part 2: Oceanic salinity, Metrologia 53, R12–R25, https://doi.org/10.1088/0026-1394/53/1/R12, 2016.

Pawlowicz, R., McDougall, T.J., Feistel, R., and Tailleux, R.: An historical perspective on the development of the Thermodynamic Equation of Seawater – 2010, Ocean Sci., 8, 161–174, https://doi.org/10.5194/os-8-161-2012 , 2012.

Pawlowicz, R., Wright, D.G., and Millero, F.J.: The effects of biogeochemical processes on oceanic conductivity/salinity/density relationships and the characterization of real seawater, Ocean Sci. 7, 363–387, https://doi.org/10.5194/os-7-363-2011, 2011.

Peters-Lidard, C.D., Hossain, F., Leung, L.R., McDowell, N., Rodell, M., Tapiadore, F.J., Turk, F.J., and Wood, A.: 100 Years of Progress in Hydrology, American Meteorological Society, https://doi.org/10.1175/AMSMONOGRAPHS-D-18-0019.1, 2019.

Phillips, C. and Foster, M.J.: Cloudiness, in: Blunden, J., Boyer, T., and Bartow-Gillies, E. (eds.): State of the Climate in 2022, Bull. Amer. Meteor. Soc. 104, S60–S61, https://doi.org/10.1175/2023BAMSStateoftheClimate.1, 2023.

Pierrehumbert, R.T.: Principles of Planetary Climate, Cambridge University Press, Cambridge, 2010.

Planck, M.: Vorlesungen über die Theorie der Wärmestrahlung, Johann Ambrosius Barth, Leipzig, Germany, 1906.

Pollack, H.N., Hurter, S.J., and Johnson, J.R.: Heat Flow from the Earth's Interior: Analysis of the Global Data Set, Reviews of Geophysics 30, 267–280, https://doi.org/10.1029/93RG01249, 1993.

Prigogine, I.: Etude Thermodynamique des Phénomènes Irreversibles (These, Bruxelles 1945), Desoer, Liege, Belgium, 1947.

Prigogine, I. : Time, structure, and fluctuations (Nobel Lecture, 8 December 1977), Science 201, 777–785, https://doi.org/10.1126/science.201.4358.777, 1978.

Randall, D.A.: Atmosphere, Clouds, and Climate, Princeton University Press, Princeton, 2012.

Rapp, D.: Assessing Climate Change. Temperatures, Solar Radiation, and Heat Balance, Springer, Cham, Switzerland, 2014.

Romps, D.M.: Exact Expression for the Lifting Condensation Level, Journal of the Atmospheric Sciences 74, 3891–3900, https://doi.org/10.1175/jas-d-17-0102.1, 2017.

Roquet, F., Madec, G., McDougall, T.J., and Barker, P.M.: Accurate polynomial expressions for the density and specific volume of seawater using the TEOS-10 standard, Ocean Modelling 90, 29-43, https://doi.org/10.1016/j.ocemod.2015.04.002, 2015.

Safarov, J., Berndt, S., Millero, F., Feistel, R., Heintz, A., and Hassel, E.: (p,ρ,T) properties of seawater: Extensions to high salinities, Deep Sea Research Part I 65, 146-156, https://doi.org/10.1016/j.dsr.2012.03.010, 2012.

Safarov, J., Berndt, S., Millero, F.J., Feistel, R., Heintz, A., and Hassel, E.P.: (p,ρ,T) Properties of seawater at brackish salinities: Extensions to high temperatures and pressures, Deep Sea Research Part I 78, 95-101, https://doi.org/10.1016/j.dsr.2013.04.004, 2013.

Safarov, J., Millero, F., Feistel, R., Heintz, A., and Hassel, E.: Thermodynamic properties of standard seawater: extensions to high temperatures and pressures, Ocean Sci. 5, 235–246, https://doi.org/10.5194/os-5-235-2009, 2009.

Sharqawy, M.H., Lienhard V, J.H., and Subair, S.M.: Thermophysical properties of seawater: a review of existing correlations and data, Desalination and Water Treatment 16, 354-380, https://doi.org/10.5004/dwt.2010.1079, 2010.

Schmidt, H., Seitz, S., Hassel, E., and Wolf, H.: The density–salinity relation of standard seawater, Ocean Sci. 14, 15–40, https://doi.org/10.5194/os-14-15-2018, 2018.

Schmidt, H., Wolf, H., and Hassel, E.: A method to measure the density of seawater accurately to the level of 10^{-6}, Metrologia 53, 770, https://doi.org/10.1088/0026-1394/53/2/770, 2016.

Seitz, S., Feistel, R., Wright, D.G., Weinreben, S., Spitzer, P., and De Bièvre, P.: Metrological traceability of oceanographic salinity measurement results, Ocean Sci. 7, 45–62, https://doi.org/10.5194/os-7-45-2011, 2011.

Seitz, S., Spitzer, P., and Brown, R.J.C.: CCQM-P111 study on traceable determination of practical salinity and mass fraction of major seawater components, Accred. Qual. Assur. 15, 9–17, https://doi.org/10.1007/s00769-009-0578-8, 2010.

Sommerfeld, A.: Thermodynamik und Statistik, Verlag Harri Deutsch, Thun, 1988.

Spänkuch, D., Hellmuth, O., and Görsdorf, U.: What Is a Cloud? Bulletin of the American Meteorological Society 103, E1894-E1929, https://doi.org/10.1175/BAMS-D-21-0032.1, 2022.

Stewart, R.H.: Introduction to Physical Oceanography, Texas A & M University: College Station, TX, USA, https://doi.org/10.1119/1.18716, 2008.

Sverdrup, H.U.: Das maritime Verdunstungsproblem, Annalen der Hydrographie und maritimen Meteorologie 64, 41-47, 1936.

Sverdrup, H.U.: On the Evaporation from the Oceans, J. Marine Research 1, 2-14, https://elischolar.library.yale.edu/journal_of_marine_research/515, 1937.

Tailleux, R.: Understanding mixing efficiency in the oceans: do the nonlinearities of the equation of state for seawater matter? Ocean Sci. 5, 271–283, https://doi.org/10.5194/os-5-271-2009, 2009.

Turner, D.R., Achterberg, E.P., Chen, C.-T.A., Clegg, S.L., Hatje, V., Maldonado, M.T., Sander, S.G., van den Berg, C.M.G., and Wells, M.: Toward a Quality-Controlled and Accessible Pitzer Model for Seawater and Related Systems, Front. Mar. Sci. 3, https://doi.org/10.3389/fmars.2016.00139, 2016.

Uchida, H., Kawano, T., Nakano, T., Wakita, M., Tanaka, T., and Tanihara, S.: An Expanded Batch-to-Batch Correction for IAPSO Standard Seawater, Journal of Atmospheric and Oceanic Technology 37, 1507–1520, https://doi.org/10.1175/JTECH-D-19-0184.1, 2020.

Uchida, H., Kayukawa, Y., and Maeda, Y.: Ultra high-resolution seawater density sensor based on a refractive index measurement using the spectroscopic interference method, Sci. Rep. 9, 1548,. https://doi.org/10.1038/s41598-019-52020-z, 2019.

Ulfsbo, A., Abbas, Z., and Turner, D.R.: Activity coefficients of a simplified seawater electrolyte at varying salinity (5–40) and temperature (0 and 25 °C) using Monte Carlo simulations, Marine Chemistry 171, 78-86, https://doi.org/10.1016/j.marchem.2015.02.006, 2015.

Unesco: Background papers and supporting data on the International Equation of State of Sea water 1980, Unesco Technical Paper Marine Science 38, UNESCO, Paris, https://www.jodc.go.jp/info/ioc_doc/UNESCO_tech/047363eb.pdf, 1981.

Valladares, J., Fennel, W., and Morozov, E.G.: Announcement: Replacement of EOS-80 with the International Thermodynamic Equation of Seawater – 2010 (TEOS-10), Deep-Sea Res. 58, 978, https://doi.org/10.1016/j.dsr.2011.07.005. Ocean Modeling 40, 1, https://doi.org/10.1016/S1463-5003(11)00154-5, 2011.

Von Rohden, C., Fehres, F., and Rudtsch, S.: Capability of pure water calibrated time-of-flight sensors for the determination of speed of sound in seawater, J. Acoust. Soc. Am. 138, 651–662, https://doi.org/10.1121/1.4926380, 2015

Von Rohden, C., Weinreben, S., and Fehres, F.: The sound speed anomaly of Baltic seawater, Ocean Sci. 12, 275–283, https://doi.org/10.5194/os-12-275-2016, 2016.

Von Schuckmann, K., Minère, A., Gues, F., Cuesta-Valero, F.J., Kirchengast, G., Adusumilli, S., Straneo, F., Ablain, M., Allan, R.P., Barker, P., et al.: Heat stored in the Earth system 1960–2020: Where does the energy go? Earth Syst. Sci. Data 15, 1675–1709, https://doi.org/10.5194/essd-15-1675-2023, 2023.

Vose, R.S., Adler, R., Gu, G., Schneider, U., and Yin, X.: Precipitation, in: Blunden, J., Boyer, T., and Bartow-Gillies, E. (eds.): State of the Climate in 2022, Bull. Amer. Meteor. Soc. 104, S57, https://doi.org/10.1175/BAMS-D-23-0090.1, 2023.

Wagner, W. and Pruß, A.: The IAPWS Formulation 1995 for the Thermodynamic Properties of Ordinary Water Substance for General and Scientific Use, J. Phys. Chem. Ref. Data 31, 387–535, https://doi.org/10.1063/1.1461829, 2002.

Wagner, W., Riethmann, T., Feistel, R., and Harvey, A.H.: New Equations for the Sublimation Pressure and Melting Pressure of H_2O Ice Ih, J. Phys. Chem. Ref. Data 40, 043103, https://doi.org/10.1063/1.3657937, 2011.

Waldmann, C., Fischer, P.F., Seitz, S., Köllner, M., Fischer, J.-G., Bergenthal, M., Brix, H., Weinreben, S., and Huber, R.: A Methodology to Uncertainty Quantification of Essential Ocean Variables, Frontiers in Marine Science 9, 1002153, https://doi.org/10.3389/fmars.2022.1002153, 2022.

Weinreben, S. and Feistel, R.: Anomalous salinity-density relations of seawater in the eastern central Atlantic, Deep–Sea Research I 154, 103160, https://doi.org/10.1016/j.dsr.2019.103160, 2019.

Weller, R.A., Lukas, R., Potemra, J., Plueddemann, A.J., Fairall, C., and Bigorre, S.: Ocean Reference Stations: Long-Term, Open-Ocean Observations of Surface Meteorology and Air–Sea Fluxes Are Essential Benchmarks, Cover. Bull. Am. Meteorol. Soc. 103, E1968–E1990, https://doi.org/10.1175/BAMS-D-21-0084.1, 2022.

Wikipedia: TEOS-10, https://en.wikipedia.org/wiki/TEOS-10, 2024.

Willett, K.M., Simmons, A.J., Bosilovich, M., and Lavers, D.A.: Surface Humidity, in: Blunden, J., Boyer, T., and Bartow-Gillies, E. (eds.): State of the Climate in 2022, Bull. Amer. Meteor. Soc., 104 (9), S49-S52, https://doi.org/10.1175/2023BAMSStateoftheCli-1262 mate.1, 2023.

WMO: Provisional State of the Global Climate 2023, World Meteorological Organization, Geneva, https://wmo.int/publication-series/provisional-state-of-global-climate-2023, 2024.

Wood, R.: Stratocumulus Clouds, Monthly Weather Review 140, 2373-2423, https://doi.org/10.1175/MWR-D-11-00121.1, 2012.

Woosley, R.J., Huang, F., and Millero, F.J.: Estimating absolute salinity (S_A) in the world's oceans using density and composition, Deep Sea Research Part I 93, 14-20, https://doi.org/10.1016/j.dsr.2014.07.009, 2014.

Wright, D.G., Feistel, R., Reissmann, J.H., Miyagawa, K., Jackett, D.R., Wagner, W., Overhoff, U., Guder, C., Feistel, A., and Marion, G.M.: Numerical implementation and oceanographic application of the thermodynamic potentials of liquid water, water vapour, ice, seawater and humid air – Part 2: The library routines, Ocean Sci. 6, 695–718, https://doi.org/10.5194/os-6-695-2010, 2010.

Wright, D.G., Pawlowicz, R., McDougall, T.J., Feistel, R., and Marion, G.M.: Absolute Salinity, ''Density Salinity'' and the Reference-Composition Salinity Scale: present and future use in the seawater standard TEOS-10, Ocean Sci. 7, 1–26, https://doi.org/10.5194/os-7-1-2011, 2011.

Wüst, G.: Die Verdunstung auf dem Meere, Veröffentlichungen des Instituts für Meereskunde an der Universität Berlin, Neue Folge, A. Geographisch-naturwissenschaftliche Reihe 6, 1–95, 1920.

You, X.: Oceans break heat records five years in a row. The heat stored in the world's oceans increased by the greatest margin ever in 2023, Nature 625, 434-435, https://doi.org/10.1038/d41586-024-00081-0, 2024.

Yu, L.: Global Variations in Oceanic Evaporation (1958–2005): The Role of the Changing Wind Speed, J. Climate 20, 5376-5390, https://doi.org/10.1175/2007JCLI1714.1, 2007.

Zhang, W., Furtado, K., Wu, P., Zhou, T., Chadwick, R., Marzin, C., Rostron, J., and Sexton, D.: Increasing precipitation variability on daily-to-multiyear time scales in a warmer world, Science Advances 7, eabf8021, https://doi.org/10.1126/sciadv.abf8021, 2021.